AD-A136 063 ADVANCED STRAIN-GAGE PRESSURE TRANSDUCER(U) GOULD INC OXNARD CA MEASUREMENT SYSTEMS DIV J DELMONTE ET AL. MAR 83 AFWAL-RR-82-2009 F33615-78-C-2064 1/1

UNCLASSIFIED F/G 13/8 NL

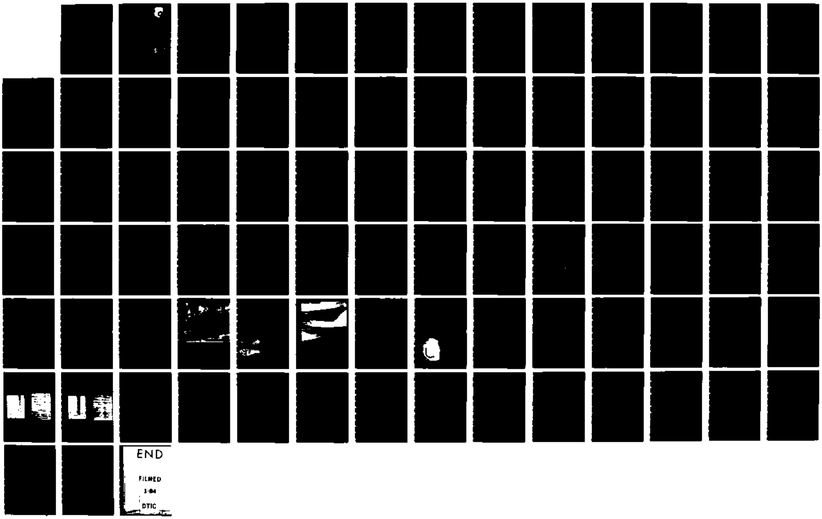

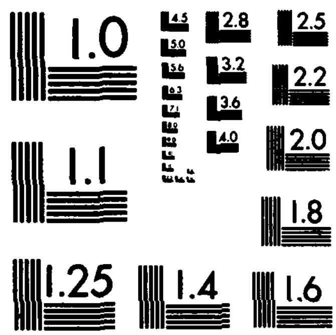

MICROCOPY RESOLUTION TEST CHART
NATIONAL BUREAU OF STANDARDS-1963-A

AFWAL-TR-82-2009

ADVANCED STRAIN-GAGE PRESSURE TRANSDUCER

GOULD, INC.
MEASUREMENT SYSTEMS DIVISION
2230 STATHAM BOULEVARD
OXNARD, CALIFORNIA 93033

MARCH 1983

FINAL REPORT FOR PERIOD OCTOBER 1978 - MARCH 1983

APPROVED FOR PUBLIC RELEASE; DISTRIBUTION UNLIMITED

AERO PROPULSION LABORATORY
AIR FORCE WRIGHT AERONAUTICAL LABORATORIES
AIR FORCE SYSTEMS COMMAND
WRIGHT-PATTERSON AIR FORCE BASE, OHIO 45433

This technical report has been reviewed and is approved for publication.

MARTIN F. HUFFMAN
Project Engineer

LESTER L. SMALL
TAM, Controls & Diagnostics

FOR THE COMMANDER

H. I. BUSH
Director, Turbine Engine Division
Aero Propulsion Laboratory

Unclassified

SECURITY CLASSIFICATION OF THIS PAGE (When Data Entered)

REPORT DOCUMENTATION PAGE

READ INSTRUCTIONS BEFORE COMPLETING FORM

1. REPORT NUMBER AFWAL-TR-82-2009	2. GOVT ACCESSION NO. AD-A136063	3. RECIPIENT'S CATALOG NUMBER
4. TITLE (and Subtitle) ADVANCED STRAIN-GAGE PRESSURE TRANSDUCER		5. TYPE OF REPORT & PERIOD COVERED Final Report for Period October 78 - March 83
		6. PERFORMING ORG. REPORT NUMBER
7. AUTHOR(s) Julian Delmonte, Harry Albaugh Daniel S. Baker Charles B. Spence		8. CONTRACT OR GRANT NUMBER(s) F33615-78-C-2064
9. PERFORMING ORGANIZATION NAME AND ADDRESS Gould, Inc., Measurement Systems Division 2230 Statham Boulevard Oxnard CA 93033		10. PROGRAM ELEMENT, PROJECT, TASK AREA & WORK UNIT NUMBERS 62203F, 30660384
11. CONTROLLING OFFICE NAME AND ADDRESS Aero Propulsion Laboratory (AFWAL/POTC) Air Force Wright Aeronautical Laboratories (AFSC) Wright-Patterson AFB OH 45433		12. REPORT DATE March 1983
		13. NUMBER OF PAGES 69
14. MONITORING AGENCY NAME & ADDRESS(if different from Controlling Office)		15. SECURITY CLASS. (of this report) Unclassified
		15a. DECLASSIFICATION/DOWNGRADING SCHEDULE

16. DISTRIBUTION STATEMENT (of this Report)

Approved for Public Release; Distribution Unlimited

17. DISTRIBUTION STATEMENT (of the abstract entered in Block 20, if different from Report)

18. SUPPLEMENTARY NOTES

19. KEY WORDS (Continue on reverse side if necessary and identify by block number)

Pressure Sensors
Instrumentation
Engine Controls
Diagnostics

20. ABSTRACT (Continue on reverse side if necessary and identify by block number)

Gould, Inc., has developed new strain gage deposition and lead wire attachment processes that have shown significant promise for improved accuracy, higher reliability, and lower cost when applied to strain gage pressure transducers now being used in gas turbine control and diagnostic systems. This report summarizes work efforts to experimentally identify and to validate, via bench tests, the benefits of these new fabrication processes. The results of static accuracy, temperature and pressure cycling, acceleration, vibration, thermal and mechanical shock, and humidity testing are discussed.

DD FORM 1 JAN 73 1473 EDITION OF 1 NOV 65 IS OBSOLETE

Unclassified

SECURITY CLASSIFICATION OF THIS PAGE (When Data Entered)

SUMMARY

The contract objective was to incorporate new developments in thin film strain gage deposition processes and lead wire attachment processes into a new, more accurate, more reliable, and lower cost pressure transducer. To accomplish this objective, four (4) prototype pressure transducers were built using a newly developed Evolution III beam design (see Figures 4 and 5) and parallel-gap welding techniques to attach gold leads to the desposited thin film circuit and adjacent printed circuit board (see Figure 4). The Evolution III beam layout utilizing long deposited runners made it possible to attach the gold leads to the stationary end of the sensing beam (see Figure 4). With the Evolution III beam design, the gold lead wires were made significantly shorter than those used on the older vapor deposited beam design (compare Figures 3 and 4), thereby increasing the natural frequency of the gold lead wires. Because the shorter gold leads can tolerate a more severe vibration environment, the transducer's reliability and useful life are increased.

Two (2) of the four (4) pressure transducers were subjected to rigorous bench testing including pressure overload, temperature cycling, static acceleration, mechanical shock, sine vibration, humidity, pressure cycling, thermal shock, and pressure-step time response. The above bench tests were designed to determine how the prototype units would perform when used in jet engine control/ diagnostic systems applications.

The remaining two (2) prototype transducers were submitted to Air Force Wright Aeronautical Laboratories for on-engine test and evaluation. These two (2) prototype units were returned to Gould MSD following the on-engine testing for recalibration and evaluation to determine if the units had been adversely effected by the engine test environment.

SUMMARY contd

The following is a listing of design accuracy goals, and the worst case results obtained from the four (4) prototype units:

ACCURACY

	DESIGN GOALS	PROTOTYPE PERFORMANCE (WORST CASE)
Non-linearity	±.15% F.S.	+.181% F.S.
Hysteresis	0.1% F.S.	.081% F.S.
Repeatability	0.1% F.S.	.042% F.S.
Thermal Effects		
Zero Shift	±.005% F.S./°F	-.0021 to +.0027% F.S./°F
Sensitivity	±.005% F.S./°F	-.0012 to +.0005% F.S./°F
Overload (150% F.S.)		
Zero Set	±0.1% F.S.	.024% F.S.

(See Tables 5 and 6 and Figures 21 and 22 for more detailed data).

As can be seen from the above data, the only design goal that was not attained was the non-linearity goal of ±.15% F.S.

Gould MSD and GLEER Laboratories are presently conducting research and development efforts to improve the new sputtered thin film deposition process. Currently, a state-of-the-art, 350 ohm resistance bridge strain gage operating at temperatures in excess of 300°F is not available. However, recent research developments utilizing alternate films are encouraging.

PREFACE

This report was prepared by the Measurement Systems Division of Gould Inc., for the Air Force Wright Aeronautical Laboratories under contract F33615-78-C-2064. This report describes research and development efforts to design, fabricate, and bench test strain gage pressure transducers that incorporate advanced strain gage deposition and lead wire attachment processes.

Mr. Charles B. Spence was the project engineer for Gould Inc. Mr. Lester L. Small of the Aero Propulsion Laboratory was the program manager for the Air Force.

The authors wish to gratefully acknowledge the valuable contributions made by the following Gould personnel:

Mr. A. Wells, Mr. R. Kodama, and Mr. G. Mowes for lead wire bonding investigations.

Dr. B. Bolker, Mr. R. Gump, Mr. D. Koneval, and Mr. D. Baker for the gage sputtering investigations.

Mr. L. Gonzales and Mr. M. Mizushima for construction and testing of prototype hardware.

TABLE OF CONTENTS

FRONT MATTER

SECTION	PAGE
LIST OF ILLUSTRATIONS	iv
LIST OF TABLES	vi
GLOSSARY OF TERMS	vii
SUMMARY	x

BODY OF REPORT

I.	INTRODUCTION	1
II.	BACKGROUND - HOW THE GOULD PRESSURE TRANSDUCER WORKS	2
III.	TASK I - NEW THIN FILM SPUTTERED DEPOSITION COMPOSITION AND GOLD LEAD WIRE ATTACHMENT VALIDATION	4
	1. New Evolution III Beam Validation	4
	2. Gold Lead Attachment Tests	6
	a. Thermocompression Ball and Stitch Bonding	6
	b. Ultrasonic Ball Bonding	7
	c. Parallel-Gap Welding	9
	d. Gold Lead Attachment Conclusions	10
	3. Prototype Fabrication and Validation	12
	a. Prototype Mechanical Design	12
	b. Prototype Electrical Circuit Design	13
	c. Prototype Initial Design Validation Test Results	14

TABLE OF CONTENTS contd

SECTION	PAGE
IV. TASK II - DETAILED PROTOTYPE BENCH TESTING	15
1. Pressure Overload Test	18
a. Requirement	18
b. Test Method	18
c. Results	18
2. Temperature Cycling Test	19
a. Requirement	19
b. Test Method	19
c. Results	20
3. Static Acceleration Test	20
a. Requirement	20
b. Test Method	21
c. Results	21
4. Mechanical Shock Test	22
a. Requirement	22
b. Test Method	22
c. Results	23
5. Sine Vibration Test	24
a. Requirement	24
b. Test Method	25
c. Results	25
6. Humidity Test	26
a. Requirement	26
b. Test Method	26
c. Results	26

TABLE OF CONTENTS contd

SECTION	PAGE
IV. TASK II - DETAILED PROTOTYPE BENCH TESTING contd	
7. Pressure Cycling Test	27
a. Requirement	27
b. Test Method	27
c. Results	27
8. Thermal Shock Test	27
a. Requirement	27
b. Test Method	28
c. Results	28
9. Pressure-Step Response Time	29
a. Requirement	29
b. Test Method	29
c. Results	30
V. TASK III - POST ON-ENGINE TEST RECALIBRATION OF PROTOTYPE TRANSDUCERS	30
1. Pre and Post On-Engine Test Data Comparison	31
VI. CONCLUSIONS	32

LIST OF ILLUSTRATIONS

FIGURE NUMBER AND TITLE	PAGE
Figure 1 - Cross-Sectional View of Prototype (Model PA8228-20) built for Wright-Patterson	35
Figure 2 - Top View of Thin Film Strain Gage Beam as Assembled in Prototypes	36
Figure 3 - Detailed View of Typical Vapor Deposited Thin Film Beam Configuration	37
Figure 4 - Evolution III Beam Configuration	38
Figure 4A - Detailed Cross-Sectional View of Thin Film (Sputtered)	39
Figure 5 - Isometric View of the Evolution III Beam	40
Figure 5A - Prototype Wiring Diagram	41
Figure 6 - Thermocompression Ball and Stitch Bonding Process	42
Figure 7 - Thermocompression Ball and Stitch Bonding Pictorial Examples	43
Figure 8 - Ultrasonic Bonding Strength vs. Deformed Wire Width	44
Figure 9 - Plastic Deformation of Wire (Ultrasonic Bonding)	44
Figure 10 - Pictorial Example of Ultrasonic Bonding	44
Figure 11 - Ultrasonic Bonding Wedges	45
Figure 12 - Parallel-Gap Welding	46
Figure 13 - Wire Ribbon Pull Test Results	47
Figure 13A - Ribbon Pull Data	48
Figure 14 - Dimensional Outline of PA8223 Prototype Transducers	49
Figure 15 - Electrical Test Circuit	50
Figure 16 - Definition of Axes	51
Figure 17 - Basic Pressure Test Circuit	52
Figure 18 - Thermal Shock Data	53

FIGURE NUMBER AND TITLE	PAGE
Figure 19 - Pressure Step Response Test Prototype Serial Number 8049, 0 to 60 psia range	54
Figure 20 - Pressure Step Response Test Prototype Serial Number 4446, 0 to 20 psia range	55
Figure 21 (a) - Pre and Post On-Engine Test: Static Accuracy Comparison (Prototype # 8020, 0 to 60 psia range)	56
Figure 21 (b) - Pre and Post On-Engine Test: Zero and Span Characteristics (Prototype # 8020, 0 to 60 psia range)	57
Figure 21 (c) - Pre and Post On-Engine Test: Thermal Error Band Comparison (Prototype # 8020, 0 to 60 psia range)	58
Figure 22 (a) - Pre and Post On-Engine Test: Static Accuracy Comparison (Prototype # 4387, 0 to 20 psia range)	59
Figure 22 (b) - Pre and Post On-Engine Test: Zero and Span Characteristics (Prototype # 4387, 0 to 20 psia range)	60
Figure 22 (c) - Pre and Post On-Engine Test: Thermal Error Band Comparison (Prototype # 4387, 0 to 20 psia range)	61

LIST OF TABLES

TABLE NUMBER	TITLE	PAGE
Table 1	Initial Design Validation Test Results (Prototype # 4387)	63
Table 2	Initial Design Validation Test Results (Prototype # 8020)	64
Table 3	Initial Design Validation Test Results (Prototype # 4446)	65
Table 4	Initial Design Validation Test Results (Prototype # 8049)	66
Table 5	Basic Performance Test Results (Prototype # 4446)	67
Table 6	Basic Performance Test Results (Prototype # 8049)	68
Table 7	Static Acceleration Test Results (Prototype # 4446 and # 8049)	69

GLOSSARY OF TERMS:

Absolute Pressure

The pressure measured relative to zero pressure measured in pounds per square inch absolute (psia).

Acceleration Error

The maximum difference, at any measurand value within the specified range. between readings taken with and without the application of specified constant acceleration along specified axes at room conditions.

Acceleration Sensitivity

The difference between the output at zero acceleration and the output measured at a given steady-state acceleration. In pressure transducers it is usually indicated as percentage of full-scale output per 'g'. It may be expressed as the output difference under acceleration at zero pressure stimulus or at some other value of pressure stimulus.

Accuracy

The ratio of the error to the full scale output, or the ratio of the error to the output expressed as a percent.

Compensation

Provision of a supplemental device or special materials to counteract known sources of error.

Calibration

Known values of the measurand are applied while the transducer output is observed or recorded. The calibration data provide information pertaining to the non-linearity and hysteresis characteristics of the transducer.

GLOSSARY OF TERMS: contd

Diaphragm

A sensing element consisting of a membrane placed between two volumes. The membrane is deformed by the pressure differential applied across it.

End Points

The outputs at the specified upper and low limits of the range.

End-Point Linearity

Non-linearity errors expressed as deviations from a straight line drawn between the end points.

End-Point Sensitivity

The algebraic difference in electrical output between the maximum and minimum values of the measurand.

Error

The algebraic difference between the indicated value and the true value of the measurand. It is usually expressed in percent of the full-scale output or in percent of the output reading of the transducer.

Excitation

The external electrical voltage and/or current applied to a transducer for its proper operation.

Full Scale

Total stimulus interval over which the instrument is intended to operate. Also, the output of the device over this interval.

Full Scale Output

The algebraic difference between the end points.

Full Scale Sensitivity

Same as full scale output.

GLOSSARY OF TERMS: contd

Hysteresis

The maximum difference in output at any given measurand value within the specified range, when the value is approached first with increasing and then with decreasing measurand.

Insulation Resistance

The resistance measured between specified insulated portions of a transducer when a DC voltage is applied at room conditions.

Non-Linearity

The deviation of a calibration curve from a specified straight line.

Measurand

A physical quantity, property, or condition which is measured (for this report, the measurand is pressure).

Output

The electrical signal, produced by a transducer, which is a function of the measurand.

Overpressure

Pressure applied in excess of the rated range of a pressure transducer.

Range

The spectrum of measurand values which exist between the upper and lower limits of the transducer's measuring capability.

Repeatability

The ability of a transducer to reproduce output readings when the same measurand value is applied to it repeatedly, under the same conditions, in the same direction.

Static Accuracy

See calibration.

Static Calibration

See calibration.

I. INTRODUCTION

The following is a "Final Technical Report" submitted in compliance with Contract F33615-78-C-2064 between Air Force Wright Aeronautical Laboratories and Gould Inc., Measurement Systems Division (Gould MSD). The contract objective was to incorporate improvements in thin film strain gage deposition methods and gold lead attachment techniques into the basic design of strain gage pressure transducers, thereby improving the accuracy, reliability, and lowering unit cost. Efforts under this contract centered on validation testing of a new deposition pattern (see Figures 3 and 4) and lead-wire attachment techniques designed to increase transducer life and improve transducer performance when used in jet engine control/diagnostic applications (i.e. high 'g', high frequency vibration environment).

The purpose of this "Final Technical Report" is to describe research and development efforts (Tasks I, II, and III) conducted by Gould MSD in compliance with the contract. First, Gould MSD conducted an engineering effort to fabricate, and bench test validate, a strain gage deposition pattern and lead-wire attachment process suitable for strain gage pressure transducer incorporation. Using the improved strain gage pattern and best gold lead attachment process, four (4) prototype pressure transducers were built and initial design validation testing was concluded (Task I). Two (2) of the prototype transducers were subjected to further bench testing to identify performance characteristics and limitations (Task II). (See Test Procedure 1053.) Finally, the two (2) remaining transducers were piggyback engine tested to determine on-engine suitability for control/diagnostic system applications (Task III).

I. INTRODUCTION contd

The following paragraphs will first present a brief description of how the Gould MSD pressure transducer works, and then describe how Tasks I, II, and III were implemented utilizing Gould's proprietary sputtered thin film process to produce an improved pressure transducer for use in jet engine control/diagnostic systems applications.

II. BACKGROUND - HOW THE GOULD PRESSURE TRANSDUCER WORKS

The Gould-Statham pressure transducer discussed here measures pressure by means of a diaphragm, linkage pin, beam and deposited strain gage sensing element (see Figure 1).

When pressure is applied to the transducer through the pressure cap, the stainless steel diaphragm is displaced by an amount directly proportional to the applied pressure (see Figure 1). This displacement is transmitted by a linkage pin to a bending beam. The beam is fixed at one end and loaded by the linkage pin at the other end, but free to deflect at the loaded end. The linkage pin applies the force to be measured perpendicularly to the median plane of the beam causing stress reversals on one surface of the beam (see Figure 1 view AA). Since the beam is symmetrical, the values of the compressive and tensile strain are equal.

The thin film strain gages are deposited directly onto the beam over the high tensile and compressive stress points. The strain gages are electrically connected into a four (4) leg active Wheatstone bridge having two tension elements and two compression elements. When a voltage is applied to the bridge, a differential voltage proportional to the pressure is generated across the bridge (see Figures 5 and 5A).

The thin film strain gage process uses techniques similar to those used in the manufacture of electronic microcircuitry. A metal substrate (bending beam) is precision polished to a mirror finish to provide the proper surface for the thin film coating. The polished parts are thoroughly cleaned and placed in a high vacuum chamber. A ceramic layer is deposited on the metal substrate to provide electrical insulation for the strain gages. Then the resistor material and gold layers are deposited. The deposited beams are then removed from the vacuum chamber and, using photolighographic techniques, the bridge resistor patterns and gold runners are defined. (See Figures 4 and 4A.) The gold ribbon lead wires are attached to make the connection from the bridge to the stand off terminals on an adjacent frame (i.e. Printed Circuit Board, see Figure 2). The bending beam assembly is protected in a hermetically sealed cavity formed by the diaphragm and the vacuum case (see Figure 1). The transducer unit assembly is evacuated and sealed in order to assure a stable reference pressure. All mechanical joints are continuous electron beam welds. Electrical feedthroughs are via ceramic seal stainless steel pins. These design features ensure a reliable hermetic seal with no measurable leakage rate.

Compensation resistors are installed to provide desired performance characteristics throughout the temperature range in which the transducer will operate (see Figure 5A, View 'C').

III. TASK I - NEW THIN FILM SPUTTERED DEPOSITION CONFIGURATION AND GOLD LEAD - WIRE ATTACHMENT VALIDATION

As of the award date of this contract, October 16, 1978, Gould Laboratories Electrical and Electronics Research, (GLEER Labs.), had developed a new sputtered thin film deposition process proprietary to Gould Inc. GLEER Labs had also defined a new deposition geometry to facilitate connecting gold leads to the thin film deposited strain gage circuit at the stationary end of the sensing beam (see Figure 4, "Evolution III Beam").

Task I as defined under Air Force Contract F33615-78-C-2064, consisted of three parts:

1. Validation testing of the new "Evolution III" sputtered thin film beam geometry (see Figure 4).
2. Evaluation of three gold-lead attachment techniques to determine the best suited bonding process to use in pressure transducer design.
3. Fabrication of four (4) prototype pressure transducers and performance initial testing to verify performance characteristics of Evolution III beam and gold-lead wire attachment processes.

The following three sections will discuss specific activities conducted by Gould MSD in conjunction with GLEER Labs to complete Task I as defined above.

1. New Evolution III Beam Validation

Figure 3 shows a standard thin film vapor deposit/shadow mask beam configuration. Note that this beam design has gold leads attached to the active, movable, end of the sensing beam. One focus under Task I of this contract was to test validate the new Evolution III beam design developed by Gould Inc.

III. TASK I - NEW THIN FILM SPUTTERED DEPOSITION CONFIGURATION AND GOLD LEAD WIRE ATTACHMENT VALIDATION contd

1. New Evolution III Beam Validation contd

The Evolution III Beam design enables the gold lead wires to be attached to the stationary end of the beam and thereby allow the use of shorter gold leads that do not move when the pressure sensing end of the beam moves. Before the development of the Gould sputtered thin film deposition process, it was not economically feasible to attach the gold leads to the fixed end of the beam because long runners (see Figure 4 and 5) were beyond the practical limits of the vapor deposition techniques.

The gold wire leads used in the Evolution III Beam design are significantly shorter than those used in the vapor deposit/shadow mask design beam (see Figures 3 and 4). The shorter lead lengths increase the natural frequency of the leads. Because the leads have a higher natural frequency, and because the leads do not move when pressure is applied to the transducer, the overall transducer design can tolerate more severe vibration environments and higher 'g' loadings, thereby increasing unit life.

Figure 4A shows a cross-sectional view of the thin film deposition layers. Validation tests revealed that the contact resistance was a limiting factor for the new Evolution III Beam design. Specifically, the resistance across the interface between the deposited gold lead runners and the strain gage resistor material changes with time and temperature.

The effects of contact "aging" are only significant at higher temperatures (above 300°F) or at low bridge resistance levels (350 ohm bridge). Therefore, for the purposes of this contract, a 5500 ohm bridge was selected. Four (4) prototype pressure transducers (two 0 to 20 psia and two 0 to 60 psia) were built for further evaluation testing of the Evolution III Beam. The results of these tests will be presented under the discussion of Task II.

III. <u>TASK I - NEW THIN FILM SPUTTERED DEPOSITION CONFIGURATION AND GOLD LEAD WIRE ATTACHMENT VALIDATION</u> contd

1. New Evoluation III Beam Validation contd

It should be noted here that Gould is engaged in company funded on-going research to develop a 350 ohm bridge with high gage factor, high accuracy, and long term stability in 300° to 600°F environments.

2. Gold Lead Attachment Tests

The second focus of activity under Task I was to test and evaluate three gold lead bonding techniques and select the bonding process most suited to Gould's pressure transducer application. The three bonding processes tested were:

1) Thermocompression ball and stitch bonding.

2) Ultrasonic ball and stitch bonding.

3) Parallel-gap resistance welding.

The next few paragraphs will first describe each bonding process separately, then a discussion of how the best bonding technique for Gould's application was selected follows.

a. Thermocompression Ball and Stitch Bonding

Thermocompression ball and stitch bonding is a widely used semiconductor bonding technique. A fine gold wire (usually .001" to .00125" diameter) is fed down through the capillary bore (see Figure 6). A small bore hydrogen cutoff torch is used to melt the wire and, by surface tension, form a ball 2 to 3 times the wire diameter (see Step 1 of Figure 6). The capillary tool is lowered to the bonding pad surface and, with the application of heat and pressure, a "ball bond" is formed (see Figure 6, Step 2 and Figure 7).

III. TASK I - NEW THIN FILM SPUTTERED DEPOSITION CONFIGURATION AND GOLD LEAD WIRE ATTACHMENT VALIDATION contd

2. Gold Lead Attachment Tests contd

a. Thermocompression Ball and Stitch Bonding contd

The capillary tool is then raised with the wire bond to the pad surface and wire is fed out of the capillary as it is positioned over another lead bonding pad (see Step 3 of Figure 6).

The capillary tool is then lowered to the bonding pad and, with application of heat and pressure, a "stitch bond" is made (see Step 4 of Figure 6).

After making the stitch bond, the capillary tool is raised, allowing wire to feed out, then a wire clamp is activated just above the capillary tool; the capillary tool is further raised, causing the wire to rupture and break at the bond without disturbing the lead bond weldment (see Figure 7 and Step 4 of Figure 6). To complete the process, the hydrogen torch is used again to form a ball on the end of the wire, preparatory to the next bonding cycle.

b. Ultrasonic Ball Bonding

The greatest advantage of the ultrasonic ball bonding process is that no heat is required. In this process, a bond is achieved through the proper transmittal of ultrasonic energy under pressure to the bond interface. Consistent and reliable bonding requires optimized parameters as illustrated in the following paragraphs. The parameters to consider are power, clamping force, duration of energy application, mating of tool geometry with wire, and bonding pad surface condition.

III. TASK I - NEW THIN FILM SPUTTERED DEPOSITION CONFIGURATION AND GOLD LEAD WIRE ATTACHMENT VALIDATION contd

2. Gold Lead Attachment Tests contd

b. Ultrasonic Ball Bonding contd

Figure 8 shows the relationship of the bond pull strength, in percent of ultimate wire tensile strength, to the deformed width of the bond (see Figure 9). Three sets of curves of bond pull strength versus power, time, or clamping force an be obtained by varying one of these parameters while holding the other two constant at their optimum. Each curve is similar to, and can be related to, the curve of bond pull strength versus wire deformed width (Reference: Small Precision Tools, 28 Paul Drive, San Rafael, CA).

As each parameter is increased (i.e. power, time, or clamping force), the weldment grows stronger in lift off strength through bond growth (see Figure 10). At the same time, due to wire deformation, the transition from the wire into the weldment becomes weaker (see Figures 10 and 11). The failure mode changes from weldment failure (lift off) to wire breakage failure (see Figure 8). Maximum pull strength is at the intersection of the two failure modes (shaded area of Figure 8). Lowest reproducibility is within the lift off failure mode and within the breakage failure mode after the deformed width exceeds two times the wire diameter. Highest reproducibility is within the breakage failure mode directly after, but less than maximum pull strength of the wire alone. This is the optimum bonding region which, while not at maximum pull strength, produces maximum reproducibility consistent with high bond strength.

III. TASK I - NEW THIN FILM SPUTTERED DEPOSITION CONFIGURAITON AND GOLD LEAD WIRE ATTACHMENT VALIDATION contd

2. Gold Lead Attachment Tests contd

c. Parallel-Gap Welding

Parallel-gap welding is a resistance weld technique where two electrodes separated by a controlled gap are placed on top of the gold lead to be welded (see Figure 12). A constant, controlled voltage difference between the electrodes is induced for a specified time causing a current to flow through the gold lead, thereby heating the lead. Because the voltage is controlled and is only applied for a specified time, the heat build up in the lead is controlled so that the lead and pad melt and fuse together.

Among the techniques available for interconnecting the external gold leads to the deposited thin film circuitry and the printed circuit board pads, welding offers several advantages. These advantages include excellent mechanical strength, low electrical resistance, and outstanding environmental qualities such as high tolerance to thermal shock and elevated temperature. Suitability of the process to well defined production control is another important advantage. The parallel gap welding process has been utilized by Gould, MSD since 1967 for all its thin film lead welding requirements.

III. TASK I - NEW THIN FILM SPUTTERED DEPOSITION CONFIGURATION AND GOLD LEAD WIRE ATTACHMENT VALIDATION contd

d. Gold Lead Attachment Test Conclusions

Thermocompression ball bonding test using the Hughes Micro Pulse Thermocompression Ball Bonder (Model MCW/BB) and Unitek Micropull 3 yielded the following results:

1. Ball and stitch welds on the beam only.
   Wire failed between 16.5 to 37.2 grams.
   Failures all occurred along the wire.
2. Ball and stitch welds on the standard terminal board pad.
   Pull force to failure was 17.4 to 17.8 grams.
   Failures all occurred at the stitch weld.
3. Ball and stitch weld on gold pins.
   Pull force to failure was 20.8 grams.
   Wire failure occurred at the ball bond.

The above results were for .002 inch diameter hardened gold wire. While the attachment results using thermocompression ball and stitch bonding are acceptable, this bonding technique does not offer a significant improvement over parallel gap welding techniques currently used by Gould MSD.

In addition, thermocompression ball and stitch welding was difficult to employ because of the clogging of the capillary bore in the crucible tip. For these reasons, it was decided not to change from parallel-gap welding to thermocompression bonding.

III. TASK I - NEW THIN FILM SPUTTERED DEPOSITION CONFIGURATION AND GOLD LEAD WIRE ATTACHMENT VALIDATION contd

d. Gold-Lead Attachment Test Conclusions contd

Ultrasonic ball and stitch bonding test results using the Hughes TSB-460 Ultrasonic Wire Bonder proved to be unsatisfactory. Because of the mismatch in energy absorption between the beam substrate material (stainless steel) and the fiberglass printed circuit board backing material, it was very difficult to consistently control the bonding process. Since the ultrasonic ball and stitch bonding process is achieved through the proper transmittal of ultrasonic energy under pressure to the bond interface, and since the energy absorption levels vary significantly at the different attachment point in the Gould transducer design, it was concluded that ultrasonic bonding was not as good as parallel gap welding for this application.

The parallel gap welding process has been used extensively by Gould MSD. Pull tests conducted on a gold sputter deposited beam (i.e. gold plated) and a gold plated terminal pin yielded favorable results (see Figure 13 and 13A). Differences in pull strength between .001" X .003" annealed and cold work hardened gold ribbon wire were discernible. As can be seen from Figure 13, the average pull strength of the annealed gold ribbon wire was 25.0 grams versus 21.4 grams for "standard" cold work hardened wire of the same dimensions.

The simplicity and repeatability of parallel-gap welding were the primary reason for selecting this attachment process over thermocompression and ultrasonic bonding. Parallel-gap welding is a proven and reliable attachment method and fits well into efficient production procedures.

III. TASK I - NEW THIN FILM SPUTTERED DEPOSITION CONFIGURATION AND GOLD LEAD WIRE ATTACHMENT VALIDATION contd

3. Prototype Fabrication and Validation

On May 16, 1980, Gould MSD was authorized by Contracting Officer, A. J. Novak, Lt. USAF, to build four (4) prototype pressure transducers. The transducer configurations approved were:

Model Identification	PA8223-20 and PA8223-60
Pressure Ranges	0 to 20 psia (build two) 0 to 60 psia (build two)
Strain Gage Resistance	Evolution III Beam configuration using 5500 ohm strain gage bridge.
Gold Lead Interconnect	Gold ribbon wire .001" X .003" annealed.

Four prototype pressure transducers were built and validation testing was accomplished. The following paragraphs will discuss:

1) Prototype mechanical design
2) Prototype electrical design
3) Prototype initial design validation test results.

The four prototypes built for this contract were built using the Evolution III beam design and the parallel-gap welding procedure to attach the gold wire leads.

a. Prototype Mechanical Design

The overall pressure transducer size was as indicated in Figure 14.

III. TASK I - NEW THIN FILM SPUTTERED DEPOSITION CONFIGURATION AND GOLD LEAD WIRE ATTACHMENT VALIDATION contd

3. Prototype Fabrication and Validation contd

a. Prototype Mechanical Design contd

Model 8223-20, 0 to 20 psi range, was built using a .005 inch thick convoluted diaphragm and an Evolution III beam with a'T' dimension of .010 inches (see Figure 1). The specially designed balance between the stiffness of the diaphragm and the stiffness of the beam, results in a movement of .0015 inches of the movable end of the Evolution III beam when 20 psia is applied to the transducer.

Model 8223-60, a 0 to 60 psia unit, had a machined diaphragm .013 inches thick and a .010 inch Evolution III beam 'T' dimension (see Figure 1). Again, the balance between the diaphragm stiffness and the beam stiffness results in .0015 inch movement at the beam when 60 psia is applied to the transducer.

All other mechanical features of these prototypes are as described earlier in this report under Section II.

b. Prototype Electrical Circuit Design

All four prototypes incorporated Evolution III beams using parallel gap gold lead attachment procedures. As shown in Figure 5A, and Figure 2, View 'C', the deposited strain gages on the Evolution III beam are wired into a Wheatstone bridge. Compensation resistors are subsequently added to adjust the sensitivity and zero out the strain gage bridge (compensation resistors located in compartment pictured in Figure 1). The wiring schematic pictured in Figure 5A shows the complete circuit used in these prototype transducers.

III. TASK I - NEW THIN FILM SPUTTERED DEPOSITION CONFIGURATION AND GOLD LEAD WIRE ATTACHMENT VALIDATION contd

3. Prototype Fabrication and Validation contd

c. Prototype Initial Design Validation Test Results

The Prototype Test Plan for Task I consisted of overload stressing (150% of full scale range) and precalibration pressure cycling to determine linearity, repeatability, and hysteresis characteristics. The prototypes were then temperature and pressure cycled to determine zero and span compensation requirements.

Following temperature compensation and final transducer assembly, each prototype was tested as follows:

1) Excitation voltage 15V DC
2) Load resistance greater than 1 megohm
3) Performed a 15 point calibration run at -65°F, -40°F, 75°F, 210°F, and 250°F

The test results are tabulated in Tables 1 thru 4. As can be seen from these data, for the PA8223-20, 0 to 20 psia range:

1) Non-linearity error was +.068 to -.056% full scale (FS) maximum.
2) Hysteresis error was +.051% full scale maximum.
3) Repeatability error was -.016% full scale maximum.
4) Thermal span error was -.0012 to +.0005% FS/°F.
5) Thermal zero error was from +.0027 to -.0017% FS/°F.

For the PA8223-60, 0 to 60 psia range, the data showed the following performance:

1) Non-linearity error was +.179% full scale (FS) maximum.
2) Hysteresis error was +.05% full scale (FS) maximum.

III. TASK I - NEW THIN FILM SPUTTERED DEPOSITION CONFIGURATION AND GOLD LEAD WIRE ATTACHMENT VALIDATION contd

3. Prototype Fabrication and Validation contd

c. Prototype Initial Design Validation Test Results contd

3) Repeatability error was from -.006 to +.004% full scale (FS) maximum.

4) Thermal span error was from -.0011 to +.0005% FS/°F.

5) Thermal zero error was from -.0021 to +.0023% FS/°F.

IV. TASK II - DETAILED PROTOTYPE BENCH TESTING

The objective of Task II was to conduct further bench testing of two (2) prototype pressure transducers to include temperature and pressure cycling, sine vibration, shock, humidity, static acceleration, response time, and thermal shock tests. These tests were designed to validate projected performance characteristics and limitations.

Coincidental, two (2) prototypes (Serial Number 4387, a 0 to 20 psia range unit, and Serial Number 8020, a 0 to 60 psia unit) were sent to Air Force Wright Aeronautical Laboratories for on-engine testing of the transducers. After engine testing, these units were returned to Gould MSD for recalibration under Task III. The other two (2) prototype transducers (Serial Number 4446, a 0 to 20 psia unit, and Serial Number 8049, a 0 to 60 psia unit) were subjected to further bench tests by Gould MSD as described under Test Procedure 1053, Revision A (see Appendix A).

To accomplish the Task II objective, Test Procedure 1053, Revision A was developed by Gould MSD and was approved on November 20, 1980 by Air Force Wright Patterson Aeronautical Laboratories (see Appendix A). Under Test Procedure 1053, Revision A, throughout the temperature range of -65°F to +250°F, the pressure transducers were to be within the accuracy requirements listed below:

Static Accuracy:

Non-linearity:	±.15% F.S. terminal
Hysteresis:	0.1% F.S.

Repeatability:

Repeatability:	0.1% F.S.

Thermal Effects:

Compensated from:	-65 to +250°F
Zero shift:	0.005% F.S./°F
Sensitivity shift:	0.005% F.S./°F

Overload Effects:

150% F.S. overload: zero set, 0.1% F.S.

Two (2) prototype pressure transducers (Serial Number 4446 and 8049) were tested for "basic performance". The test calibration method used was a fifteen (15) point pressure survey with rated power (15V DC) applied to the transducer. After connecting the transducer to a dial manometer, and the test circuit pictured in Figure 15, the transducer was placed in a temperature chamber and thermally stabilized at a given test temperature ±2°F for one hour. With the unit stabilized at the set temperature, pressure was reduced to less than 0.01 psia and the output was recorded. A fifteen (15) point calibration was then accomplished by slowly increasing the applied pressure so as to approach each pressure increment using care not to overshoot the desired setting. Similarly, when decreasing the pressure, care was taken not to undershoot the desired setting. All pressure-step outputs were recorded and are presented in columns 1 through 6 of Tables 5 and 6. (NOTE: The transducers were tested at -65°F±2°F, -40°F ± 2°F, -75°F ± 2°F, +210°F ± 2°F, and +250°F ± 2°F. "Basic repeatability" of the transducer was established by two consecutive calibrations at room temperature, 75°F).

The above described test method was used to establish the "basic performance" characteristics for each prototype (see Tables 5 and 6). Using these data as a static accuracy base line, (i.e. 15 point calibration at 75°F was termed "Initial Static Accuracy", see column 4 of Tables 5 and 6) further bench testing was conducted. After each test was completed; a 15 point calibration run was made at 75°F and the data compared to the "Initial Static Accuracy Data".

After the "Initial Static Accuracy" base line was established, the following tests were performed:

1) Pressure overload
2) Temperature cycling
3) Static acceleration
4) Mechanical shock
5) Sine vibration
6) Humidity
7) Pressure Cycling

IV. TASK II - DETAILED PROTOTYPE BENCH TESTING contd

8) Thermal shock

9) Pressure-step response time

The following paragraphs will describe how each of the above tests were accomplished and the results of each.

1. Pressure Overload Test

a. Requirement

After 150% of full scale overload, zero set will be less than .1% full scale (F.S.).

b. Test Method

The prototype transducers were connected to the test circuit pictured in Figure 15, pressure was reduced to less than .01 psia, and transducer output voltage was recorded. The units were then subjected to 150% of full scale overload pressure for two (2) minutes and their output voltage was recorded. The overload cycle was repeated three (3) times.

c. Results

Results of the overload tests are listed below:

PRESSURE (psia)	OUTPUT (mV)	
	S/N 4446 0 to 20 psia RANGE	S/N 8049 0 to 60 psia RANGE
	USED 30 psia OVERLOAD	USED 90 psia OVERLOAD
0	-.016	-.242
OVERLOAD	75.722	75.211
0	-.004	-.235
OVERLOAD	75.720	75.212
0	-.004	-.235
OVERLOAD	75.722	75.211
0	-.004	-.235c
ZERO SET AS % OF FULL SCALE	+.024% FS	+.014% FS

IV. TASK II - DETAILED PROTOTYPE BENCH TESTING contd

1. Pressure Overload Test contd

c. Results

The projected accuracy goal for this test was a zero set of less than 0.1% F.S. after application of a 150% F.S. overload. As can be seen from the data, the zero set due to overload was less than +.024% F.S. (used full scale sensitivity of 50.512 mV for S/N 4446 and 50.391 mV for S/N 8049, see column 4 of Tables 5 and 6) and is thus within specification.

2. Temperature Cycling Test

a. Requirement

After 55 temperature cycles from -65°F to +250°F, the transducers shall meet the static accuracy goals as shown in Tables 5 and 6.

b. Test Method

The transducers (Serial Numbers 4446 and 4089) were placed in a temperature test chamber. A cycle-time controller was connected to the chamber to bypass the chamber manual control. One complete cycle consisted of a one (1) hour temperature soak at -65°F, one-half (1/2) hour to change the test chamber temperature from -65°F to 250°F, a one (1) hour temperature soak at 250°F, and finally one-half (1/2) hour to bring the chamber temperature back to -65°F. Total elapsed time for one cycle was three (3) hours. The prototype transducers were subjected to 55 continuous cycles over a seven (7) day period. After temperature cycling, the transducers were subjected to a static accuracy test (at 75°F) as described earlier (i.e. 15 point calibration survey).

IV. TASK II - DETAILED PROTOTYPE BENCH TESTING contd

2. Temperature Cycling Test contd

c. Results contd

As can be seen from the data tabulated in column 7 of Tables 5 and 6 the results were:

STATIC ACCURACY REQUIRED	PROTOTYPE ACTUAL PERFORMANCE	
	S/N 4446	S/N 8049
Non-Linearity ±.15% F.S.	+.057% F.S.	+.173% F.S.
Hysteresis 0.1% F.S.	+.038% F.S.	+.040% F.S.
Zero Set (not specified)	-.099% F.S.	-.528% F.S.
NOTE: After this initial zero set taken after the thermal cycling test, the zero remained within ±.077% F.S. of the post temperature cycling test zero (see columns 7 thru 13 of Tables 5 and 6).		

The 0 to 60 psia unit, Serial Number 8049, was .031% F.S. above the goal of 0.15% F.S., for the static non-linearity requirement. However all other requirements were met by both units.

3. Static Acceleration Test

a. Requirement

The transducers shall maintain the "static accuracy" listed on Tables 5 and 6 after being subjected to a sustained acceleration of 10 g through three (3) perpendicular axes. The duration of the acceleration shall be greater than five (5) seconds and shall be repeated 10 times along each of three (3) axes (see Figure 16 for axis definition). An output variation of .05% F.S./g is permitted for the transducer during acceleration along the X axis.

3. Static Acceleration Test contd

b. Test Method

The transducers were mounted on a centrifuge along the +X axis. Rated input voltage of 15V DC was applied to the transducers and the output voltage of the transducers was recorded. The centrifuge was operated to apply 10 g's to the transducers. The 10 g acceleration was maintained for 5 to 10 seconds and the transducers output was recorded. This procedure was repeated 10 times. The units were then rotated 180° to apply acceleration in the opposite direction along the X axis. The transducers were again accelerated 10 times to 10 g's, maintaining the 10 g level for 5 to 10 seconds and recording transducer output while the units were experiencing a 10 g acceleration loading.

Next, the transducers were remounted in the Y and Z axes and the procedure was repeated.

c. Results

As can be seen from Table 7, for Serial Number 4446, a 0 to 20 psia unit, the maximum output change of -.377 mV due to 10 g acceleration loading was in the -X axis direction. Using the initial full scale sensitivity value of 50.512 mV as determined during the "initial static accuracy" tests, (see Table 5, Column 3) the maximum variation was .075% F.S./g for this unit which exceeds the goal of .05% F.S./g.

Similarly, for Serial Number 8049, a 0 to 60 psia unit, the maximum acceleration response occurred in the -X axis direction. Maximum output change during 10 g acceleration loading was -.120 mV. Using the initial sensitivity value of 50.391 mV as measured during "initial sensitivity accuracy" test, the maximum variation was .024% F.S./g for this unit.

IV. TASK II - DETAILED PROTOTYPE BENCH TESTING contd

3. Static Acceleration Test contd

c. Results contd

After the static acceleration tests described above were completed, both units were retested for static accuracy (i.e. a 15 point calibration survey at 75°F). These data are tabulated in column 8 of Tables 5 and 6. As can be seen from the data, S/N 4446 remained well within the required .15% F.S. non-linearity specification, S/N 8049 did not change significantly since the "initial static accuracy" value of +.162% F.S. non-linear.

4. Mechanical Shock Test

a. Requirement

The transducers shall be subjected to 24 impact shocks of 60 g with a time duration of not less than 10 milliseconds. Four (4) shocks shall be applied in each direction along each of three (3) mutually perpendicular axes (see Figure 16 for definition of axes). The transducers shall withstand the impact loads without permanent damage.

b. Test Method

Four (4) shock impacts of 60 g's with a duration of 10 milliseconds and a wave shape approximating a half-sine, were applied in each direction (i.e. positive and negative direction) along each of the three (3) mutually perpendicular axes (axes as defined in Figure 16, total of 24 impact shocks were applied). The shock testing was conducted by Approved Engineering Test Laboratories, Valley Division, Chatsworth, California.

IV. TASK II - DETAILED PROTOTYPE BENCH TESTING contd

4. Mechanical Shock contd

c. Results

Both prototype transducers were pressurized to 15 psia and output voltage was recorded before and after shock tests. Data is presented below:

UNIT	AXIS	OUTPUT (mV)		% F.S. CHANGE
		BEFORE	AFTER	
S/N 8049	+X	11.478	11.480	+.004% F.S.
(0 to 60 psia)	-X	11.494	11.496	+.004% F.S.
	+Y	11.487	11.485	-.004% F.S.
	-Y	11.483	11.484	+.002% F.S.
	+Z	11.495	11.493	-.004% F.S.
	-Z	11.493	11.496	+.006% F.S.
S/N 4446	+X	35.818	35.821	+.006% F.S.
(0 to 20 psia)	-X	35.887	35.887	.000% F.S.
	+Y	35.805	35.795	-.020% F.S.
	-Y	35.810	35.807	-.006% F.S.
	+Z	35.847	35.842	-.010% F.S.
	-Z	35.853	35.857	+.008% F.S.

Excitation Voltage Applied: 15V DC

Full Scale (FS) Sensitivity: S/N 8049 = 50.391 mV
S/N 4446 = 50.512 mV

IV. TASK IV - DETAILED PROTOTYPE BENCH TESTING contd

4. Mechanical Shock contd

c. Results contd

Following shock testing, both prototype units were tested for static accuracy and the data compared to the "initial static accuracy" data. As can be seen from Column 9 of Tables 5 and 6, Serial Number 4446 had a non-linearity error +.048% F.S. and hysteresis error of +.040% F.S., while Serial Number 8049 had non-linearity error of +.170% F.S. and hysteresis error of .040% F.S. Both units were well within the hysteresis requirement of .1% F.S., however Serial Number 8049, the 0 to 60 psia unit, had a non-linearity error greater than the allowed .15% F.S. However, Serial Number 8049 had a non-linearity error of +.164% F.S. during "initial static accuracy" testing and this error was virtually unchanged after shock testing.

Based on the data it was concluded that the 10 g shocks did not effect the "static accuracy" of either transducer.

5. Sine Vibration Test

a. Requirement

The transducer shall maintain calibration (i.e. static accuracy) after being vibrated at 40 g's for 3 hours in each of the three mutually perpendicular axes. An output variation of less than 0.2% F.S./g is permitted for the transducer when vibrated along each axis (see Figure 16 for axes definition).

5. Sine Vibration Test contd

b. Test Method

The transducers were mounted on a vibration exciter and 15V DC excitation voltage was applied to each transducer. The pressure port of each transducer was vented to the atmosphere. An oscilloscope was used to monitor the output from the transducers during vibration. The units were subjected to sine vibration along each axis pictured in Figure 16, at a sweep rate of one octave per minute at the frequencies and vibratory levels shown below:

FREQUENCY (cps)	VIBRATION LEVELS
5 to 88	0.10" DA
88 to 2000	40.0 g's

Resonant modes of the transducer were determined by varying the frequency of the applied vibration from 5 to 2000 cps at a 2 g level. A resonance was defined as a repeatable peak output at a specific frequency which is greater than five times the average noise output over the frequency range at the applied 'g' level.

c. Results

Both units showed no resonant modes between 5 and 2000 cps. A static accuracy test was performed on each unit after sine vibration testing (see column 10 of Tables 5 and 6) and both units exhibited the same basic accuracy (i.e. no significant change) as in their "initial static accuracy" test (see column 4 of Tables 5 and 6).

IV. TASK II - DETAILED PROTOTYPE BENCH TESTING contd

6. Humidity Test

a. Requirement

The transducer shall operate within the static accuracy requirements (see Tables 5 and 6) after exposure to 95 ± 5 percent relative humidity at 130°F for 15 days with the inlet port vented to the atmosphere.

b. Test Method

The transducers, non-operating, were placed in a chamber with humidity greater than 90%. The chamber temperature was increased to 130°F and maintained at this temperature for 15 days. At the end of 15 days, the transducers were removed from the chamber and examined for corrosion or rust and none was found. The moisture was removed from the electrical terminals by blowing nitrogen gas across the terminals. A static accuracy test (i.e. 15 point calibration survey) at 75°F was conducted within one (1) hour after removal from the humidity chamber.

c. Results

After careful inspection of each transducer, no rust or corrosion was found following humidity testing. This result was not surprising as both prototypes were built using all welded stainless steel construction and are hermetically sealed.

Results of the static accuracy test performed after removing the units from the humidity chamber are tabulated in Column 11 of Tables 5 and 6 and are essentially unchanged when compared to "initial static accuracy" data found in Column 4 of Tables 5 and 6.

7. Pressure Cycling Test

a. Requirement

After 250,000 pressure cycles from approximately 0 psia to the full rated pressure of the transducer, the unit shall meet the static accuracy requirement listed in Tables 5 and 6.

b. Test Method

The pressure port of each transducer was connected to a pneumatic pressure cycler (see Figure 17). The cycler was adjusted to provide a variation in pressure from 0.2 psia to 20 ± 2 psia at a rate of approximately 6 cycles per minute for transducer Serial Number 4446, the 0 to 20 psia unit. Similarly, the cycler was adjusted to provide a variation in pressure from .02 psia to 60 ± 0.6 psia for Serial Number 8049, the 0 to 60 psia unit. At the completion 250,000 cycles on each unit, a static accuracy test was performed on each unit.

c. Results

Static accuracy data (i.e. 15 point pressure calibration survey completed at 75°F) taken after the pressure cycling test is tabulated in Column 12 of Tables 5 and 6. As can be seen by comparing this data to the "initial static accuracy" data (see Column 4 of Tables 5 and 6), the transducers characteristics did not change after pressure cycling.

8. Thermal Shock Test

a. Requirement

The transducers shall be subjected to a thermal shock test at a constant pressure level wherein the transducer output and the transducer case temperature are continuously monitored/recorded while the case temperature is rapidly (i.e. less than 30 seconds) decreased by a 50°F step.

8. Thermal Shock Test contd

b. Test Method

Each transducer, equipped with a metal tube attached to the pressure port, was stabilized at 85°F ± 2°F in an oven for 45 minutes with rated voltage of 15V DC applied. Each transducer case was instrumented with a thermocouple to facilitate monitoring of transducer case temperature.

A dual trace recorder was used to monitor the output from the transducer and the thermocouple while the transducer was submerged in a stabilized ice-water bath. The pressure port of the transducer remained vented to the atmosphere via the metal tube attached to the pressure port. Using this method, the transducers were subjected to a 50°F step temperature change in less than 30 seconds.

c. Results

Figure 18 presents the thermal shock data from tests conducted on Serial Numbers 4446 and 8049. As can be seen from Figure 18, unit 4446, with 0 to 20 psia range, exhibited a -.55% full scale (F.S.) change in the first 1.25 minutes and then, after 6 minutes, returned to only -.25% F.S. difference from the initial 85°F stabilized output reading.

Similarly, transducer 8049, a 0 to 60 psia unit, experienced a -.65% F.S. change after .8 minutes of the thermal shock. As the transducer case thermally stabilized after 6 minutes, the transducer output returned to only a .25% F.S. change from the initial pre-thermal shock output.

IV. TASK II - DETAILED PROTOTYPE BENCH TESTING contd

8. Thermal Shock Test contd

c. Results contd

A post-thermal shock static accuracy test was run on both prototype units after the units were thermally stabilized at 75°F for one hour. Column 13 of Tables 5 and 6 tabulated the post thermal shock test static accuracy data. By comparing Columns 13 with Column 4 in Tables 5 and 6, it can be seen that no significant change occurred in the basic performance of either unit.

9. Pressure-Step Response Time

a. Requirement

The transducers shall have a time constant of less than 0.01 second. The time constant is defined as the time required for the transducer, exhibiting a first order response, to reach 63.2 percent of its normal output after being subjected to a stimulus of a step pressure change as follows:

MODEL	PRESSURE STEP
PA8223-60 (Serial Number 8049)	45 psi (60 psia to 15 psia)
PA8223-20 (Serial Number 4446)	10 psi (25 psia to 15 psia)

b. Test Method

The pressure step response time of the prototype units was obtained by applying a step pressure to the pressure port and photographing the transducer output waveform obtained on an oscilloscope.

The step pressure input was obtained by connecting the pressure port of the transducer to a fixture which had 1-1/2" opening at one end. The fixture opening was then covered by a .001 inch thick cellophane diaphragm and the fixture cavity was pressurized to a predetermined pressure above

b. Test Method

atmospheric (fixture pressurized to 60 psia for Serial Number 8049, and 25 psia for the Serial Number 4446 test). The diaphragm was then ruptured, venting the pressure port of the transducer to the atmosphere and exposing the subject transducer to a calibrated pressure step input.

c. Results

Figures 19 and 20 show the response outputs of both prototype transducers. As can be seen from the photographs in Figures 19 and 20, the response time for Serial Number 4446 was .000126 seconds and .000205 seconds for Serial Number 8049. Both units' response time was well below the .01 second allowed.

V. TASK III - POST ON-ENGINE TEST RECALIBRATION OF PROTOTYPE TRANSDUCERS

Coincidental with the accomplishment of Task II by Gould MSD, on-engine tests of two prototype transducers were completed by Air Force Wright Aeronautical Laboratories. Two transducers, serial numbers 4387 and 8020, were shipped to ASD/PMRSA Air Force Systems Command, Wright-Patterson AFB, Ohio, on 20 January 1981.

Following piggyback engine testing of both transducers, the units were returned to Gould MSD for recalibration. Recalibration was completed by 18 June 1982. A comparison of transducer performance data generated before (as shipped) engine tests and after (as returned) engine tests is presented in the following paragraphs of this report.

V. TASK III - POST ON-ENGINE TEST RECALIBRATION OF PROTOTYPE TRANSDUCERS

1. Pre and Post On-Engine Test Data Comparison

Figures 21 A, B, and C and Figures 22 A, B, and C, show a comparison of transducer characteristics before and after the jet engine tests.

Figure 21 (A) and Figure 22 (A) present static accuracy data taken at different temperature levels. As can be seen from the data, hysteresis error and non-linearity error increased only slightly after engine testing.

Figures 21 (B) and 22 (B) show before and after engine test data. Four graphs are presented in each figure. The top two graphs show how the span of the transducer changes with temperature as a % of full scale sensitivity. The lower graphs shown how the zero behaves as a function of temperature (shown in % FS). As can be seen from these graphs, the span and zero characteristics of the transducer were affected only slightly by jet engine testing.

Finally, Figures 21 (C) and 22 (C) display more before and after engine test data. The curves on the charts represent the difference (error), in % full scale, that the transducer output varies from a straight line connecting the end points (see Glossary of Terms) of the transducer output, calibrated at 75°F. As can be seen from the data, on-engine testing had little effect on the transducer performance.

VI. CONCLUSIONS

The following is a comparative listing of design accuracy goals, and the worst case results obtained from the four (4) prototype units:

STATIC ACCURACY

	DESIGN GOALS	PROTOTYPE PERFORMANCE (WORST CASE)
Non-linearity	±.15% F.S.	+.181% F.S.
Hysteresis	0.1% F.S.	.081% F.S.
Repeatability	0.1% F.S.	.042% F.S.
Thermal Effects		
Zero Shift	±.005% F.S./°F	-.0021 to +.0027% F.S./°F
Sensitivity	±.005% F.S./°F	-.0012 to +.0005% F.S./°F
Overload (150% F.S.)		
Zero Set	0.1% F.S.	.024% F.S.

(See Tables 5 and 6 and Figures 21 and 22 for more detailed information).

As can be seen from the above data, the design goal of ±.15% F.S. non-linearity was not met by Model PA8223-60, the 0 to 60 psia units.

Unfortunately the non-linearity of the zero through temperature is an inherent part of the mechanism and cannot be compensated. The only solution would be to redesign the 0 to 60 psia prototypes.

Although both transducers maintained static accuracy after the static acceleration test, S/N 4446, a 0 to 20 psia unit, exceeded the goal of .05% F.S./g with a maximum variation of .075% F.S./g along the -X axis. The high value originates from the ratio of the suspended (moving) mass of the

VI. CONCLUSIONS contd

system to it's stiffness (spring constant of the moving system). Decreasing the diameter of the link pin and diaphragm width would reduce the suspended mass. The link pins in the prototypes had large diameters to allow a stronger pin to beam weld, but considering the pressure range for which model PA8223-20 was designed to operate, the increased weld strength becomes less important.

ILLUSTRATIONS

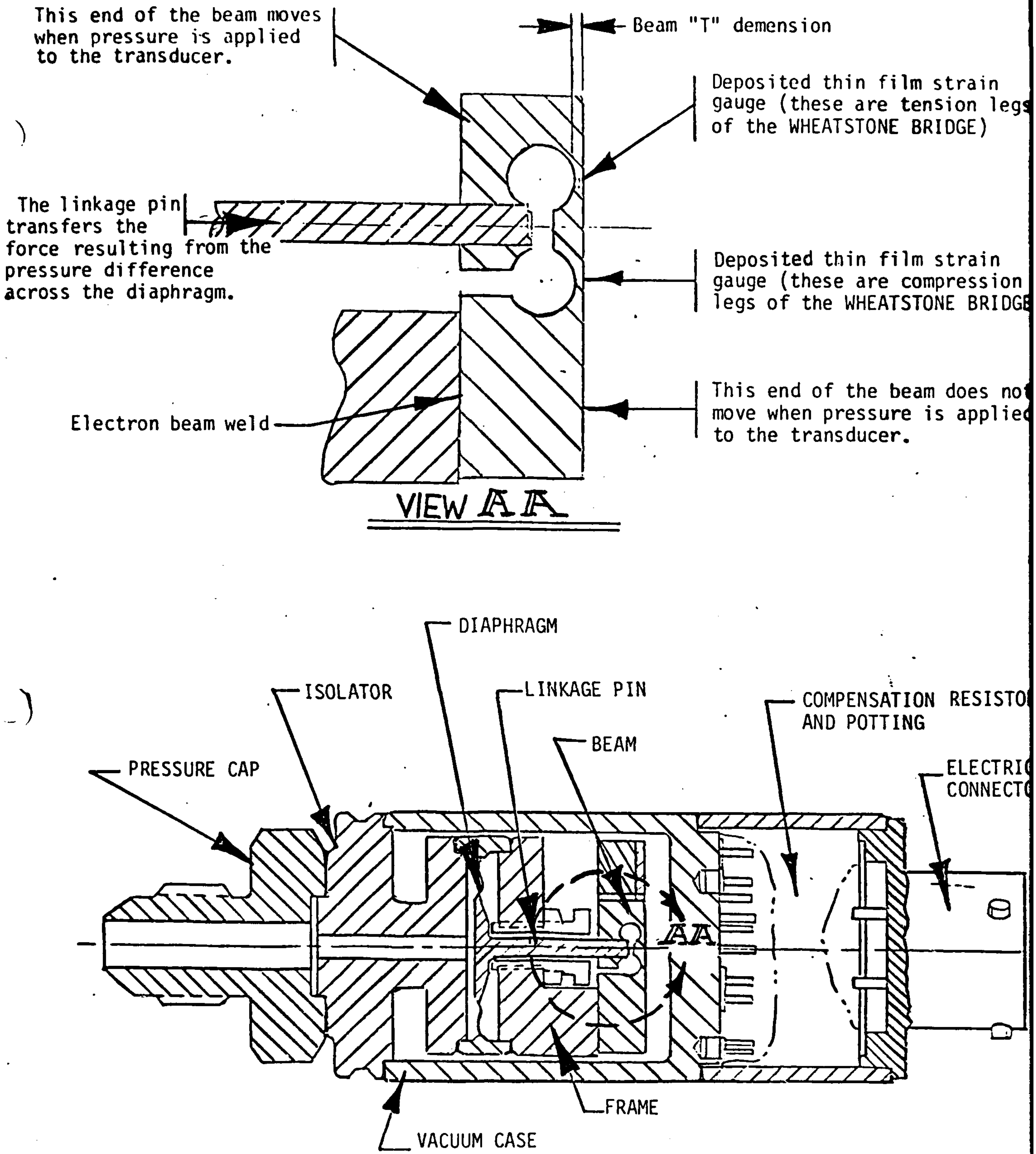

FIGURE 1

CROSS-SECTIONAL VIEW OF PROTOTYPE MODEL PA8223-20 BUILT FOR WRIGHT-PATTERSON

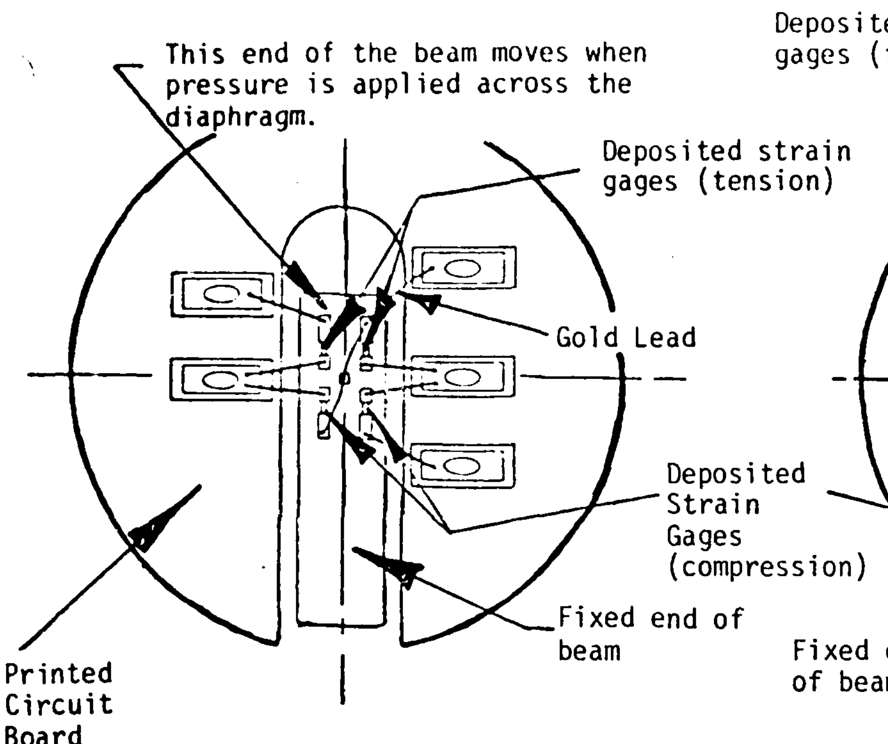

VIEW B

Transducer as wired using the Vapor Deposited thin film prosses. Note that the gold lead wires are longer than those used on the Evolution III Beam design. Also note that the gold leads are attached to the moving end of the beam. (see Figure 3 for more detail)

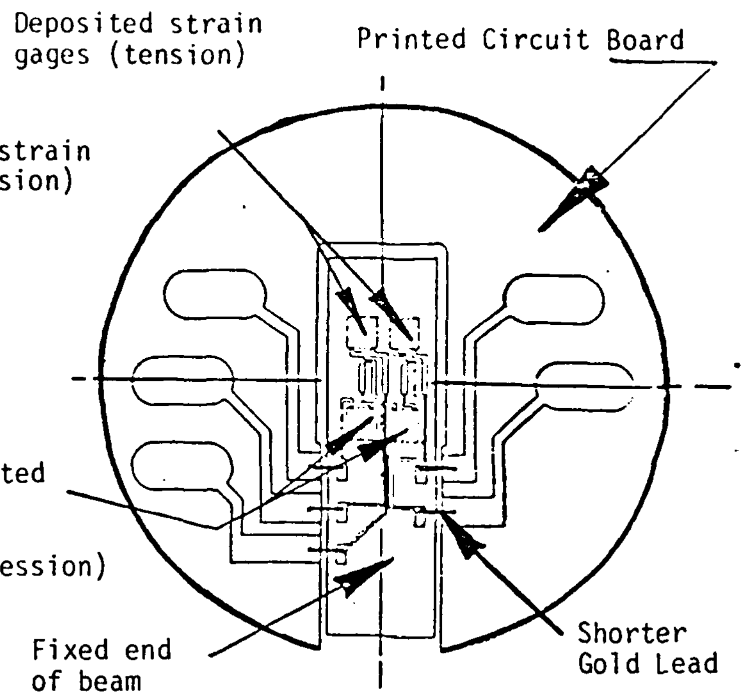

VIEW C

Transducer as wired using the new Evolution III Beam design layout. Note the gold leads are shorter and are attached to the stationary end of the beam. (see Figure 4 for more detail)

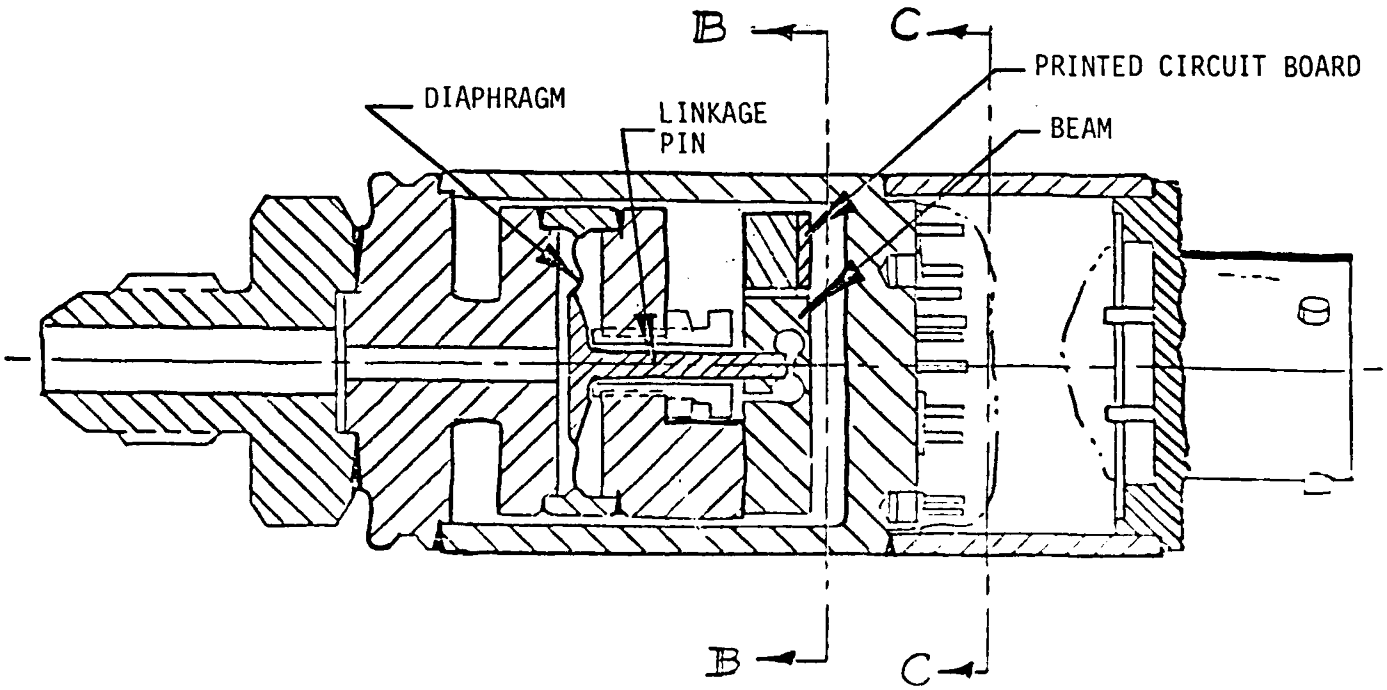

FIGURE 2

TOP VIEW OF THIN FILM STRAIN GAGE BEAM (VIEW C,USING EVOLUTION III BEAM,IS HOW PROTOTYPES WERE BUILT)

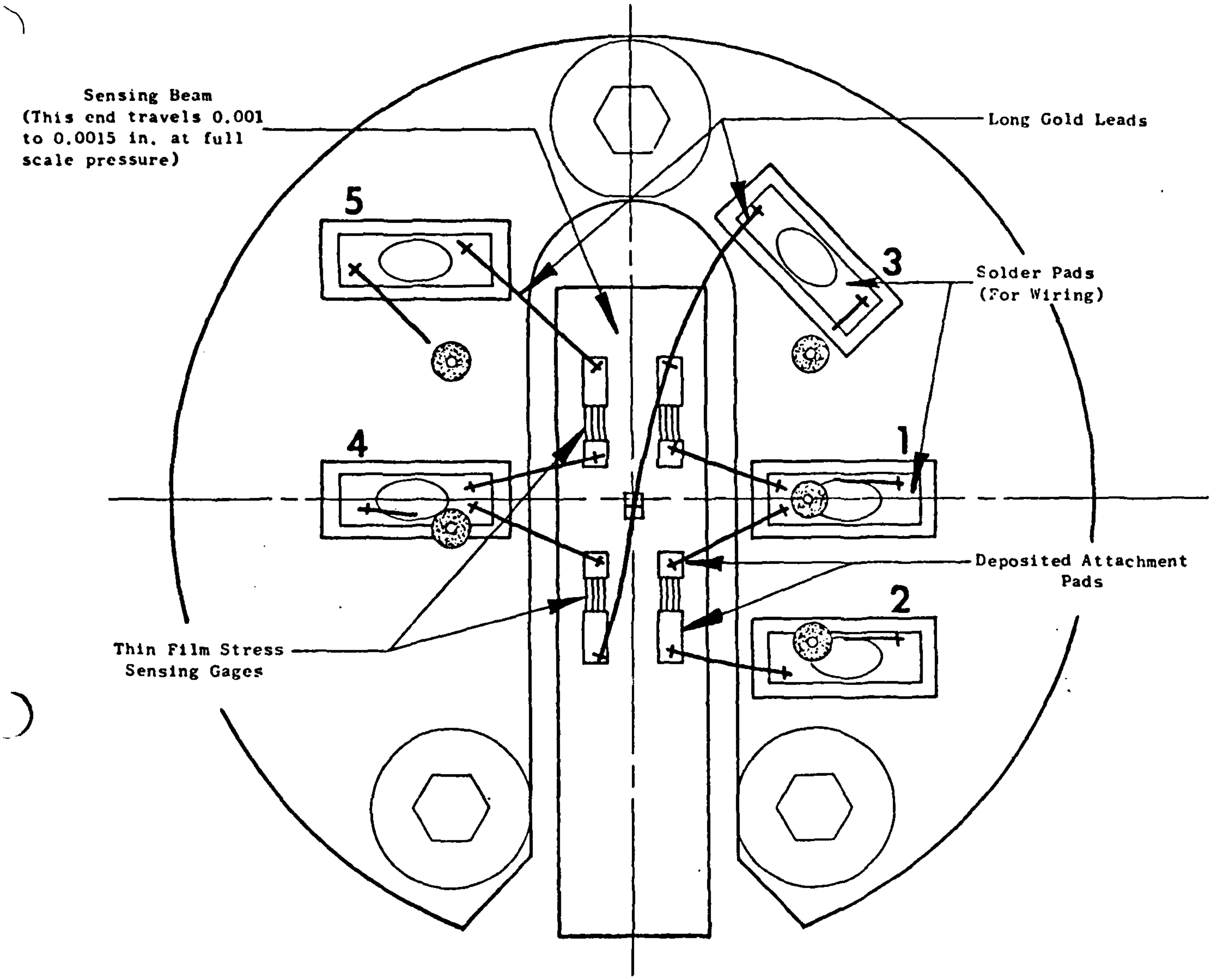

FIGURE 3

Detailed Top View of Typical Vapor Deposited Thin Film Beam Configuration

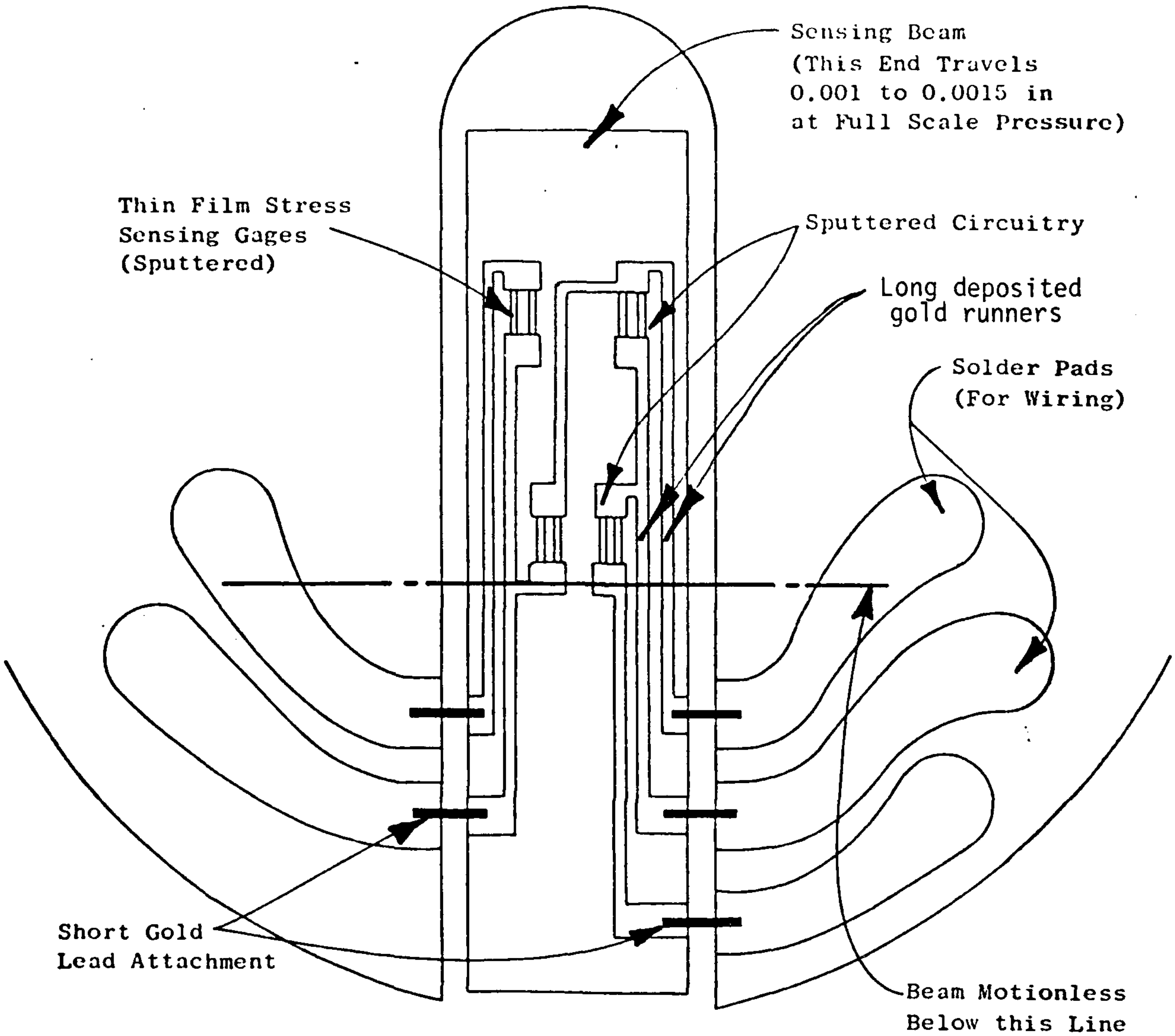

FIGURE 4
EVOLUTION III BEAM CONFIGURATION (new gold lead location)

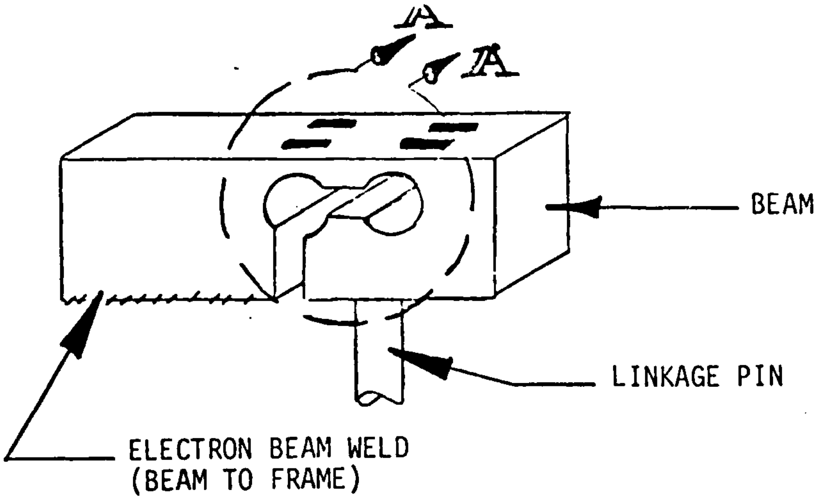

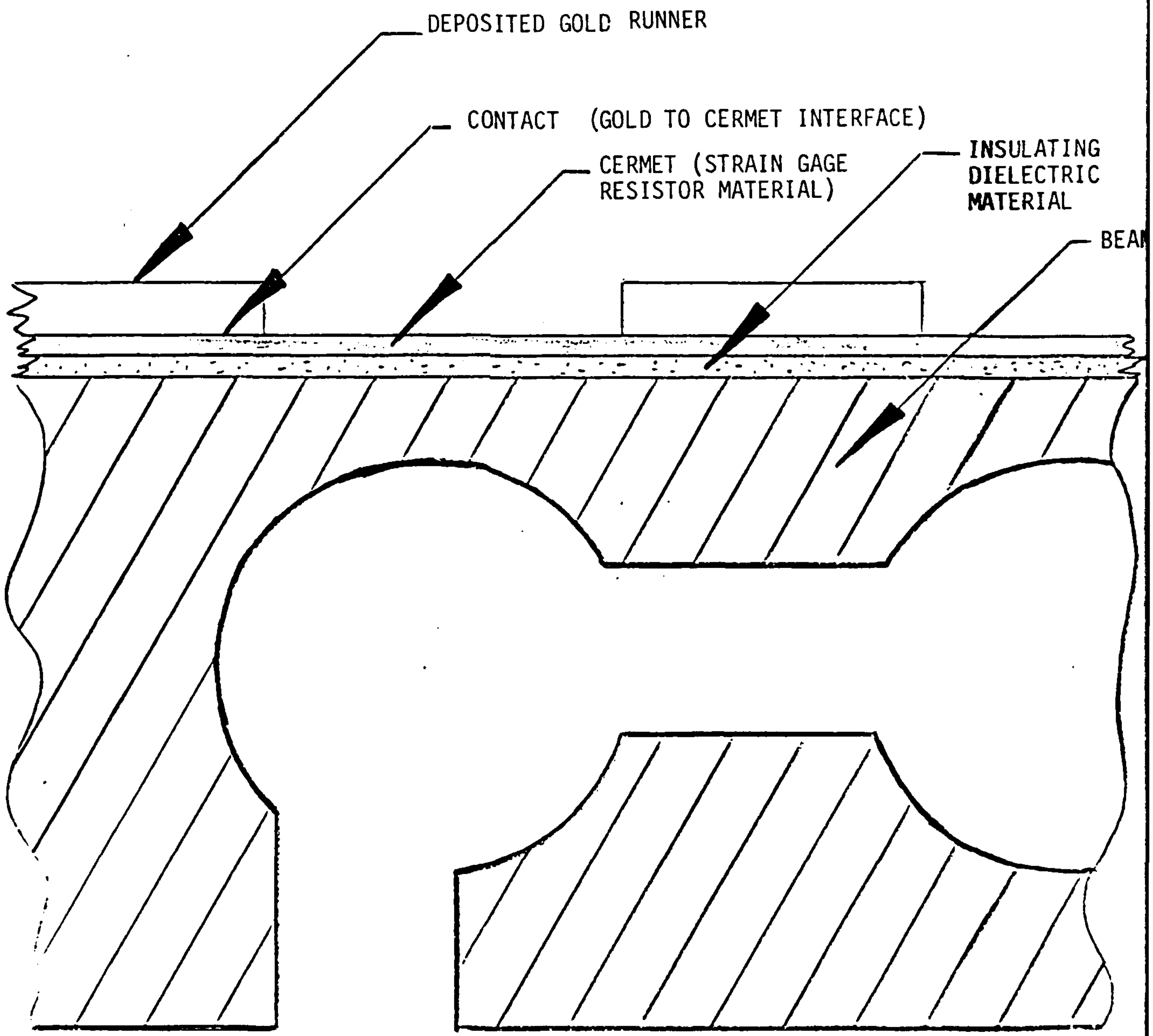

VIEW A

FIGURE 4A

DETAILED CROSS-SECTIONAL VIEW OF THIN FILM (SPUTTERED)

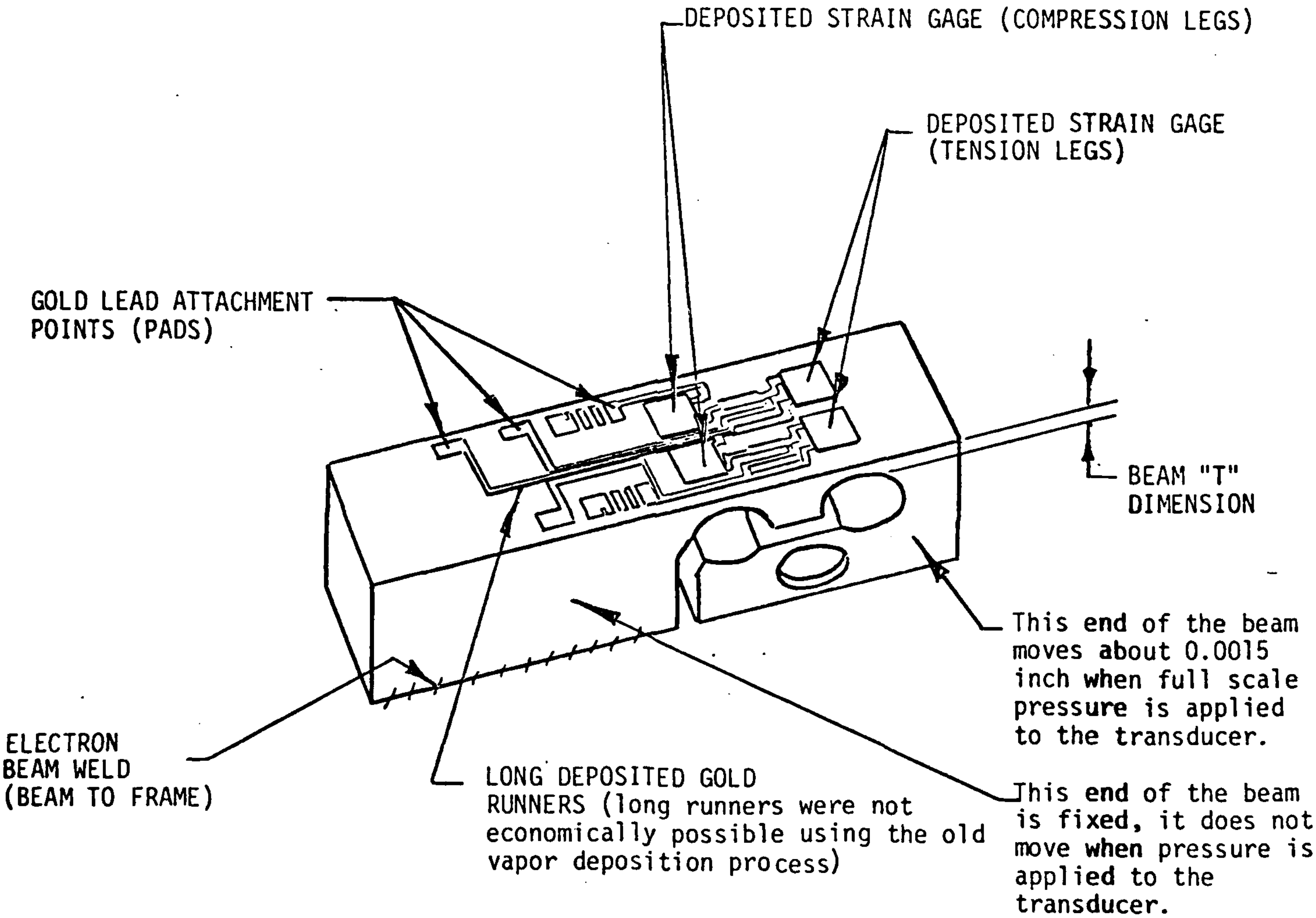

FIGURE 5

ISOMETRIC VIEW OF THE EVOLUTION III BEAM

For orientation of the two drawings below, see Figure 2, View C.

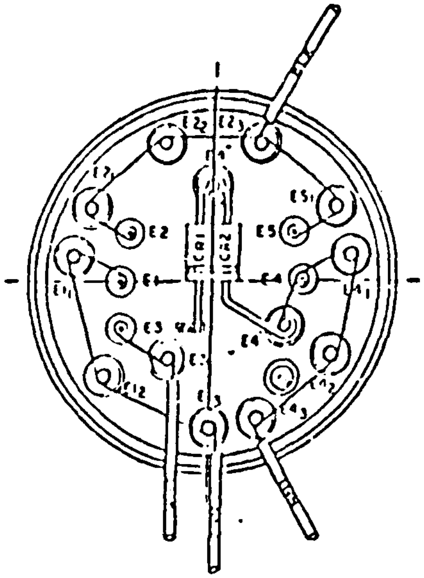

VIEW B

PRELIMINARY WIRING
(this wiring set up is used during initial temperature runs to determine the values of compensation resistors required)

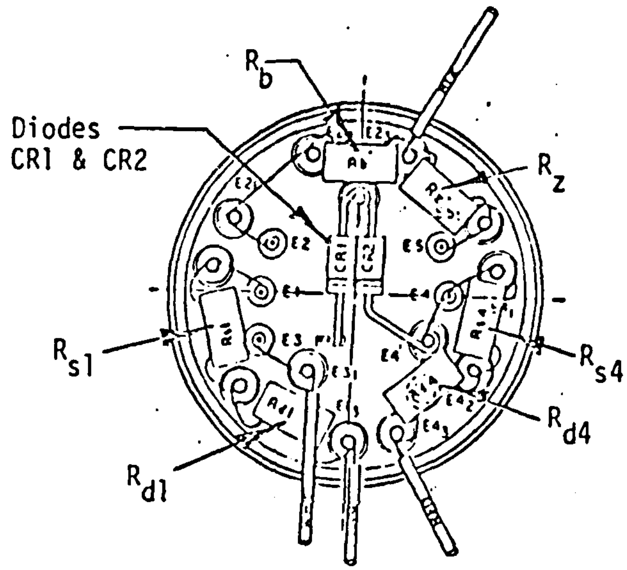

VIEW C

COMPONENT INSTALLATION
(LAYOUT SHOWN FOR REFERENCE ONLY)
(above is a drawing of a fully compensated transducer)

RESISTOR TERMINOLOGY

R_s = Span Compensation

R_d = Dropping Resistor

R_z = Zero Compensation

R_b = Bridge Balance

CR 1 & 2 = Diodes

VIEW A

Deposited strain gages wired as a WHEATSTONE BRIDGE

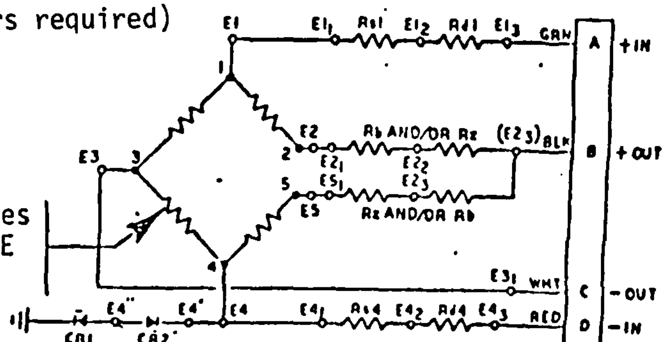

SCHEMATIC

FIGURE 5A

WIRING DIAGRAM

PA8223

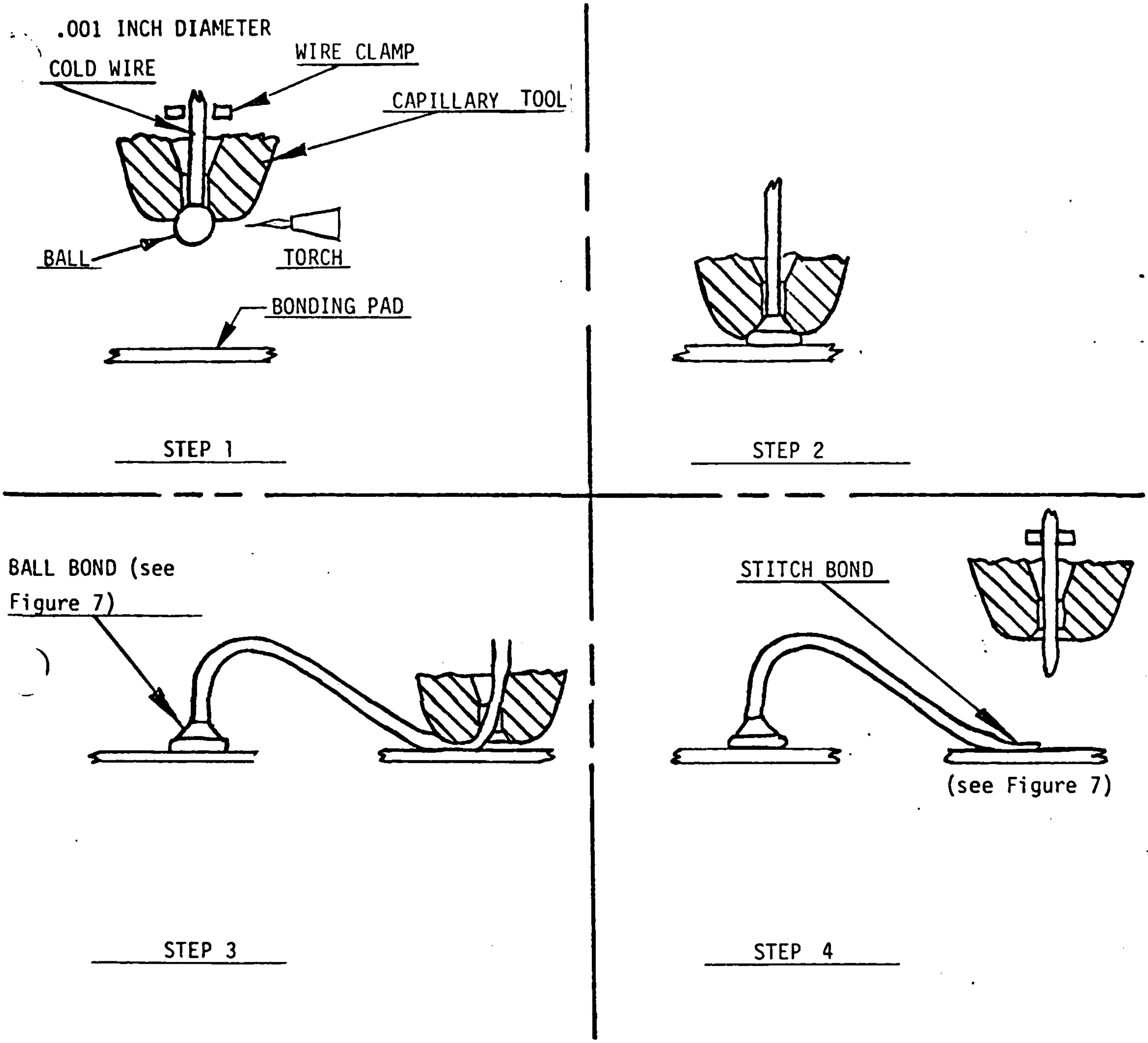

FIGURE 6
THERMOCOMPRESSION BALL
AND STITCH BONDING PROCESS

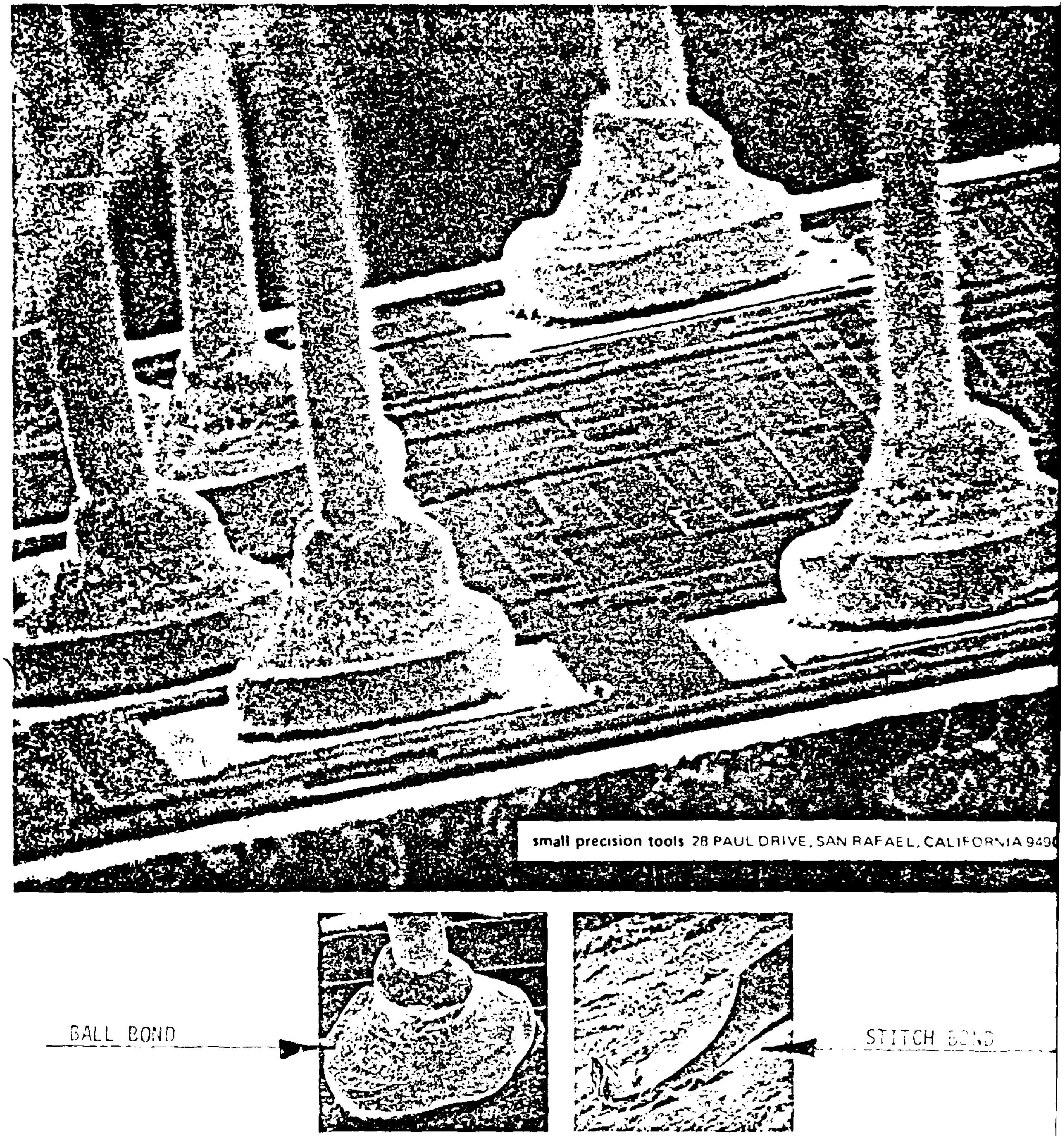

FIGURE 7

THERMOCOMPRESSION BALL

AND STITCH BONDING

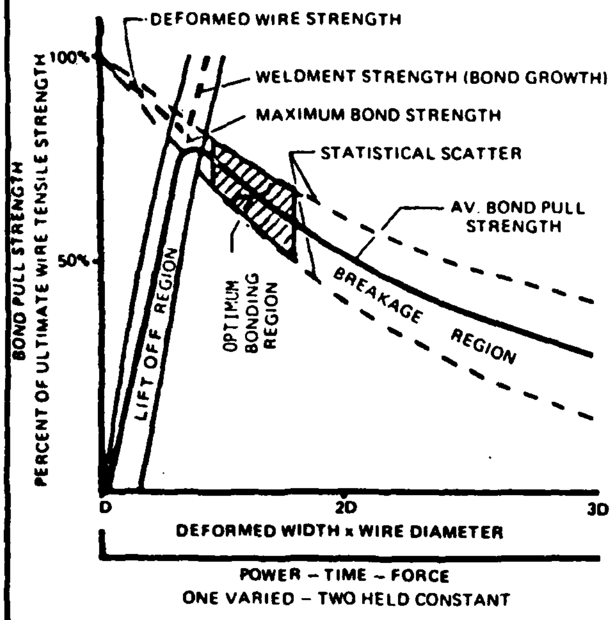

Fig. 8 - Bond Pull Strength vs. Deformed Width or Ultrasonic Power

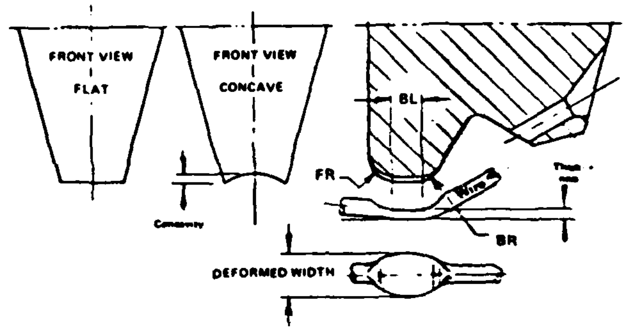

Fig. 9 - Plastic Deformation of Wire Produced by Ultrasonic Bonding

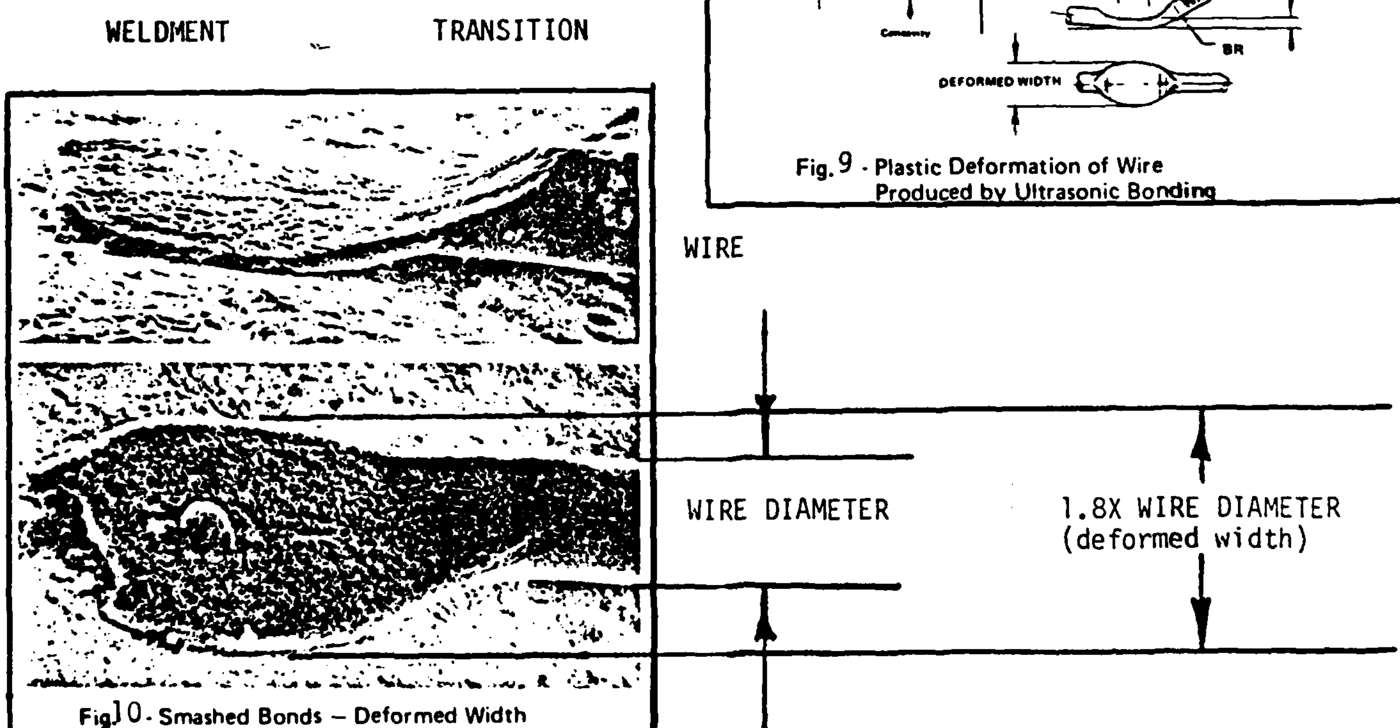

Fig. 10 - Smashed Bonds – Deformed Width Greater Than 1.8X Wire Diameter

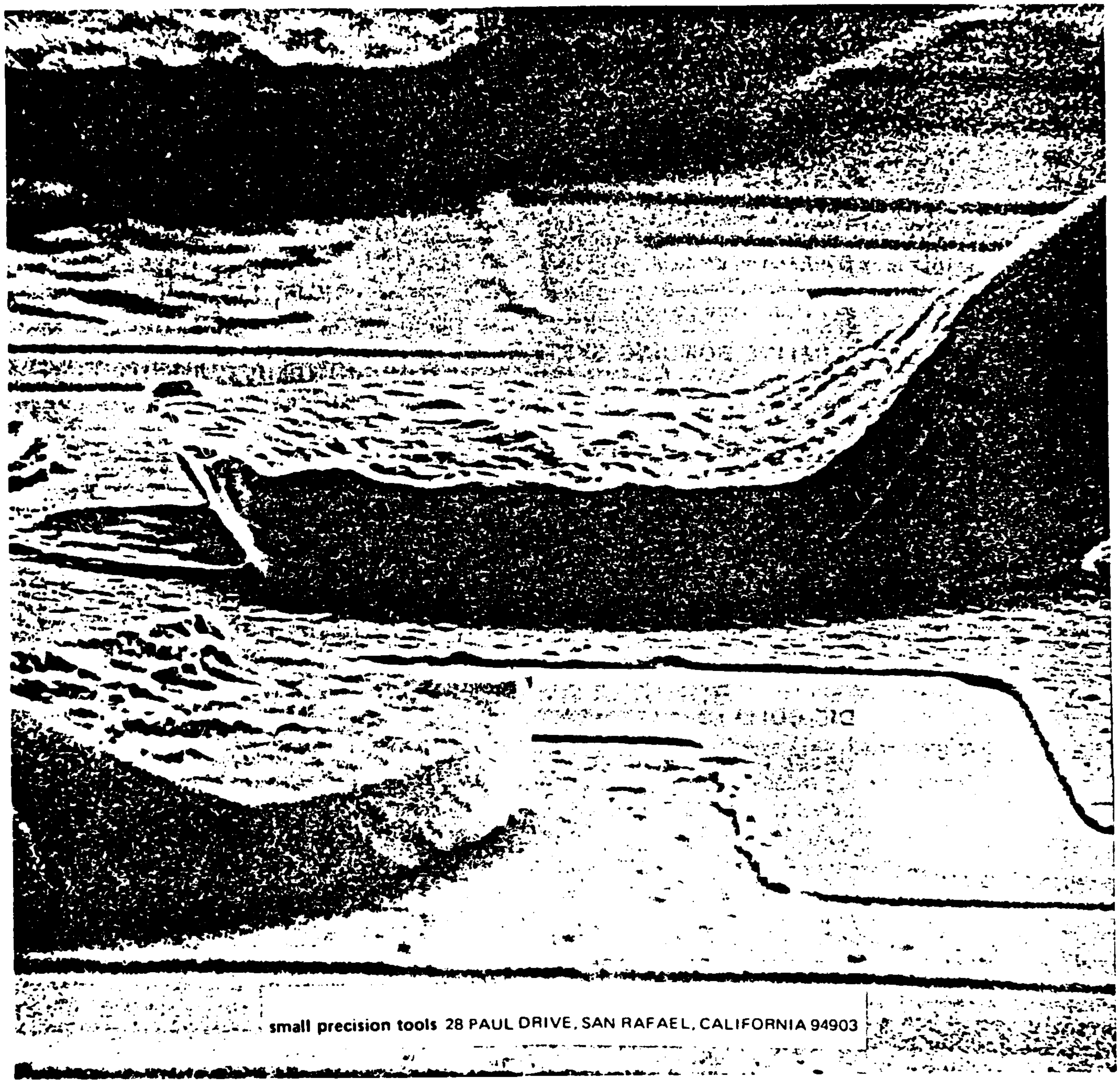

FIGURE 11

ULTRASONIC BONDING WEDGES

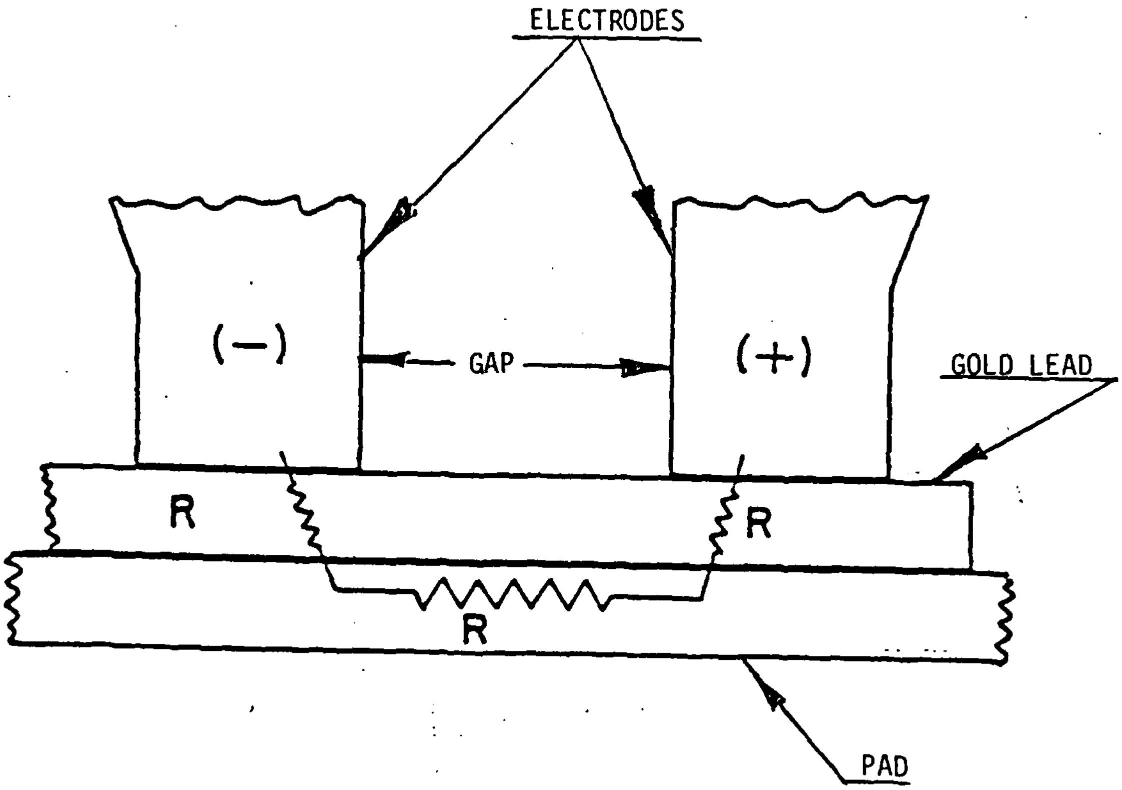

FIGURE 12

PARALLEL GAP WELDING

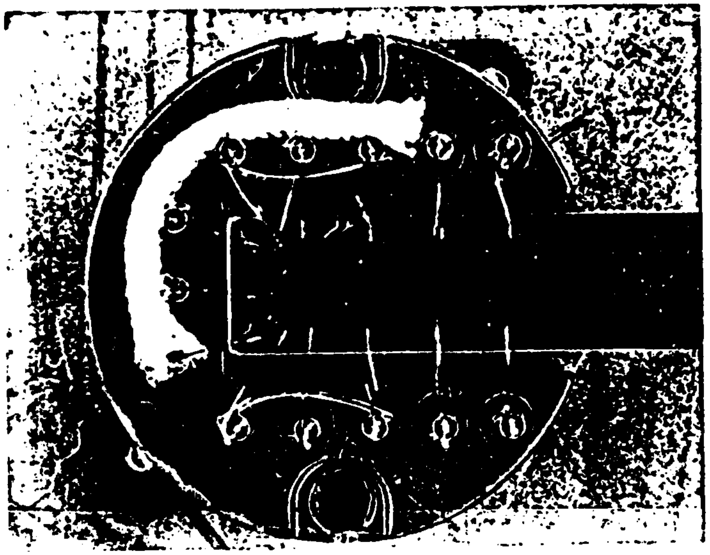

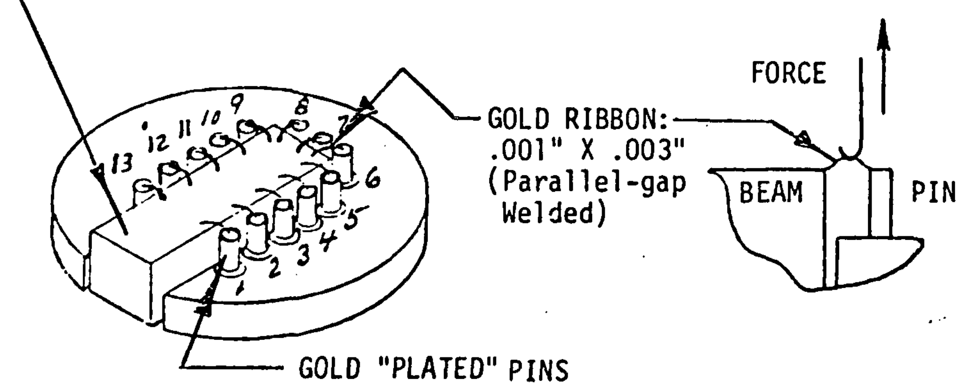

DATA SUMMARY
PULL-TO-BREAK FORCE - GRAMS - OF .001" X .003" RIBBON WIRE

	ANNEALED	STANDARD*
$\overline{X}$ AVERAGE	25.1 grams	21.4 grams
X MINIMUM	18.4 grams	16.0 grams
X MAXIMUM	28.6 grams	24.4 grams
STANDARD DEVIATION	2.00 grams	2.25 grams
FAILURES AT BEAM:	12	24
FAILURES AT PIN:	22	15
FAILURES AT CENTER OF RIBBON:	4	0

(Ultimate strength of gold ribbon, annealed, approximately 27.2 grams).

*5 to 8% elongation (cold-worked).

FIGURE 13

DATA
PULL-TO-BREAK FORCE
OF
GOLD WIRE RIBBON
.001" X .003"

ANNEALED				STANDARD			
SAMPLE NUMBER	POSITION NUMBER **	PULL STRENGTH (grams)	BREAKAGE POINT	SAMPLE NUMBER	POSITION NUMBER **	PULL STRENGTH (grams)	BREAKAGE POINT
1	1	25.4	Beam	1	1	20.5	Beam
2	2	26.3	Beam	2	2	23.8	Beam
3	3	26.1	Pin	3	3	21.4	Pin
4	4	25.6	Beam	4	4	24.4	Beam
5	5	23.7	Pin	5	5	19.6	Beam
6	6	25.6	Center	6	6	18.0	Pin
7	7	22.8	Pin	7	7	16.0	Pin
8	8	23.9	Beam	8	8	21.9	Beam
9	9	23.7	Beam	9	9	25.6	Beam
10	10	23.2	Pin	10	10	21.8	Beam
11	11	23.1	Pin	11	11	20.4	Beam
12	12	23.7	Pin	12	12	18.6	Beam
13	13	23.6	Pin	13	13	21.5	Beam
14	1	27.4	Pin	14	1	21.2	Beam
15	2	25.2	Beam	15	2	22.0	Pin
16	3	25.2	Pin	16	3	22.3	Pin
17	4	25.7	Beam	17	4	19.7	Pin
18	5	24.0	Pin	18	5	17.3	Pin
19	6	23.9	Beam	19	6	24.3	Beam
20	7	18.4	Pin	20	7	23.6	Beam
* 21	8	10.2	Pin	21	8	22.6	Pin
22	9	22.4	Pin	22	9	21.8	Pin
23	10	24.9	Pin	23	10	23.5	Beam
24	11	25.9	Center	24	11	20.7	Pin
25	12	24.3	Beam	25	12	23.9	Pin
26	13	28.1	Pin	26	13	21.7	Pin
27	1	25.9	Beam	27	1	18.0	Beam
28	2	24.2	Pin	28	2	24.0	Beam
29	3	22.6	Center	29	3	24.0	Beam
30	4	23.9	Pin	30	4	22.9	Pin
31	5	27.1	Pin	31	5	17.3	Pin
32	6	28.2	Pin	32	6	20.3	Pin
33	7	28.6	Pin	33	7	22.9	Beam
34	8	23.6	Pin	34	8	22.9	Beam
35	9	25.5	Beam	35	9	19.9	Beam
36	10	27.4	Center	36	10	20.9	Beam
37	11	25.9	Pin	37	11	22.9	Beam
38	12	27.6	Pin	38	12	19.4	Beam
39	13	26.6	Beam	39	13	22.2	Beam

* Data from the sample was omitted.
*See Figure 13 for location of position numbers.

FIGURE 13A
RIBBON PULL DATA

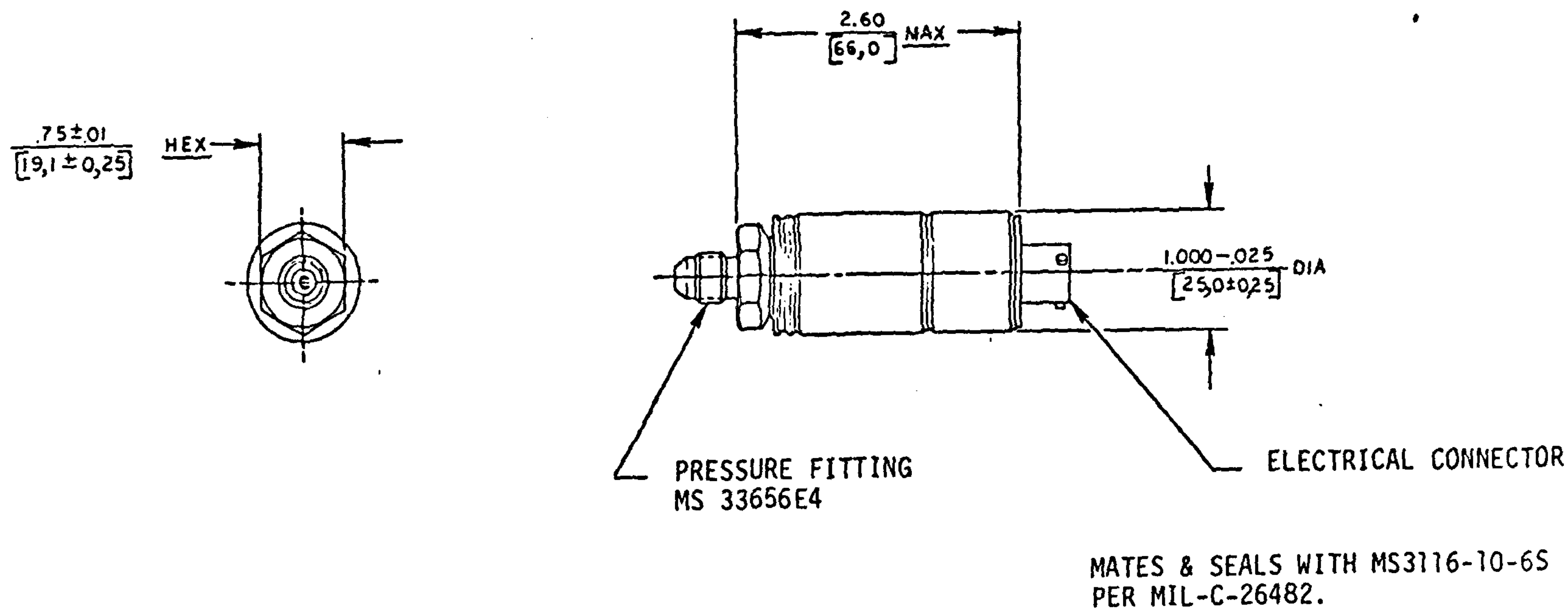

OUTLINE PA8223 PRESSURE TRANSDUCER
Dimensions are the same for the Model PA8223-60 and the PA8223-20. Only specific internal dimensions are different (see Section III 3.a. of report text).

FIGURE 14

ELECTRICAL TEST CIRCUIT

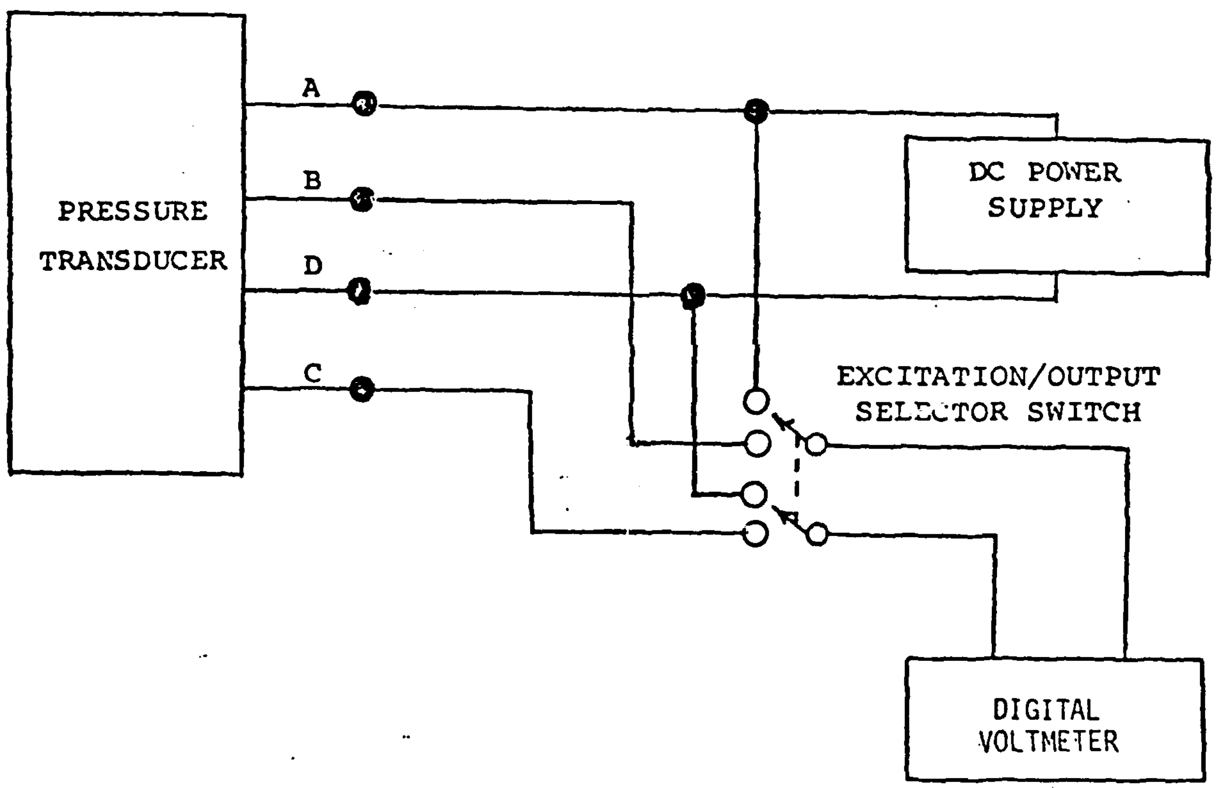

FIGURE 15

FIGURE 16

DEFINITION OF AXES AND DIRECTION

OF ACCELERATION FORCES

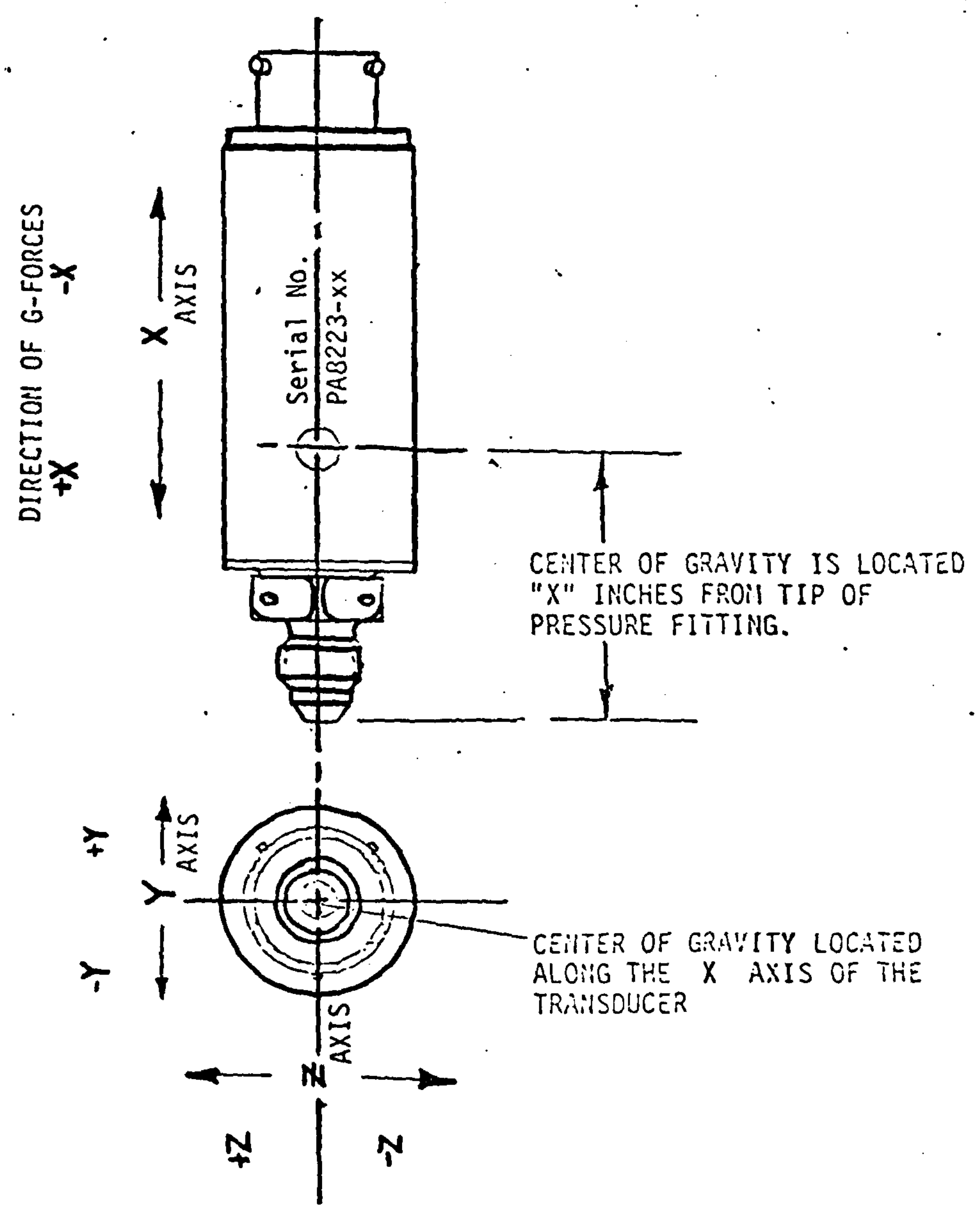

FIGURE 17

BASIC PRESSURE TEST CIRCUIT

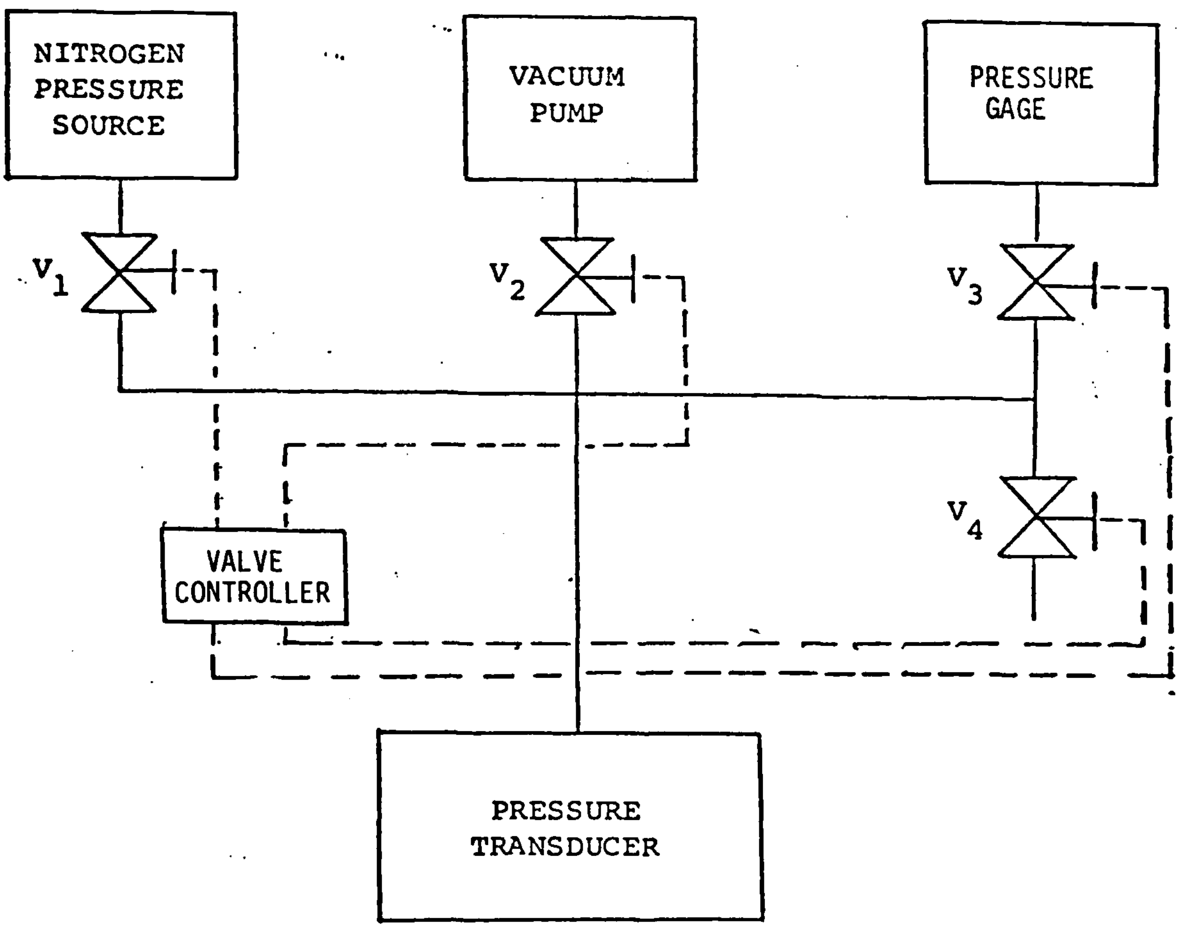

[illegible]

TEST CONDITIONS:
1: Stabilized at [illegible]°F with power applied.
2: Removed from temperature chamber and immersed in 32°F water (ice bath).
3: Test pressure: ≤ 0.01 psia.
4: Transducer and Thermocouple output monitored on strip chart recorder.

MODEL: [illegible]
S/N: [illegible]
RANGE: 0 to [illegible] psia
FS: [illegible]
LOAD: Open ckt.
T/C: Fe/Const.

TEST DATE: 04-21-81

OUTPUT vs. TIME

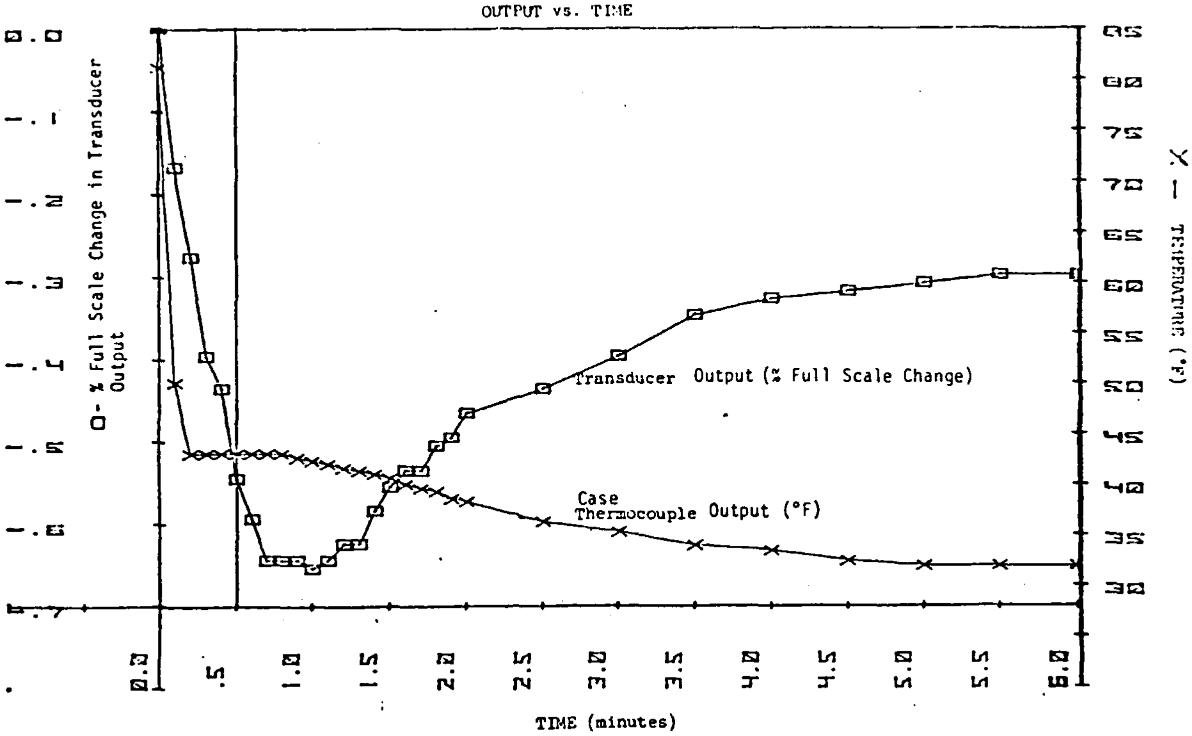

<u>THERMAL SHOCK TEST</u>

TEST CONDITIONS:
1: Stabilized at 85°F with power applied.
2: Removed from temperature chamber and immersed in 32°F water (ice bath).
3: Test pressure: ≤ 0.01 psia.
4: Transducer and Thermocouple output monitored on strip chart recorder.

MODEL: PA8223-20
S/N: 4446
RANGE: 0 to 20 psia
FS: 50.512mV/15V/20psia
LOAD: Open ckt.
T/C: Fe/Const.
TEST DATE: 04-21-81

OUTPUT vs. TIME

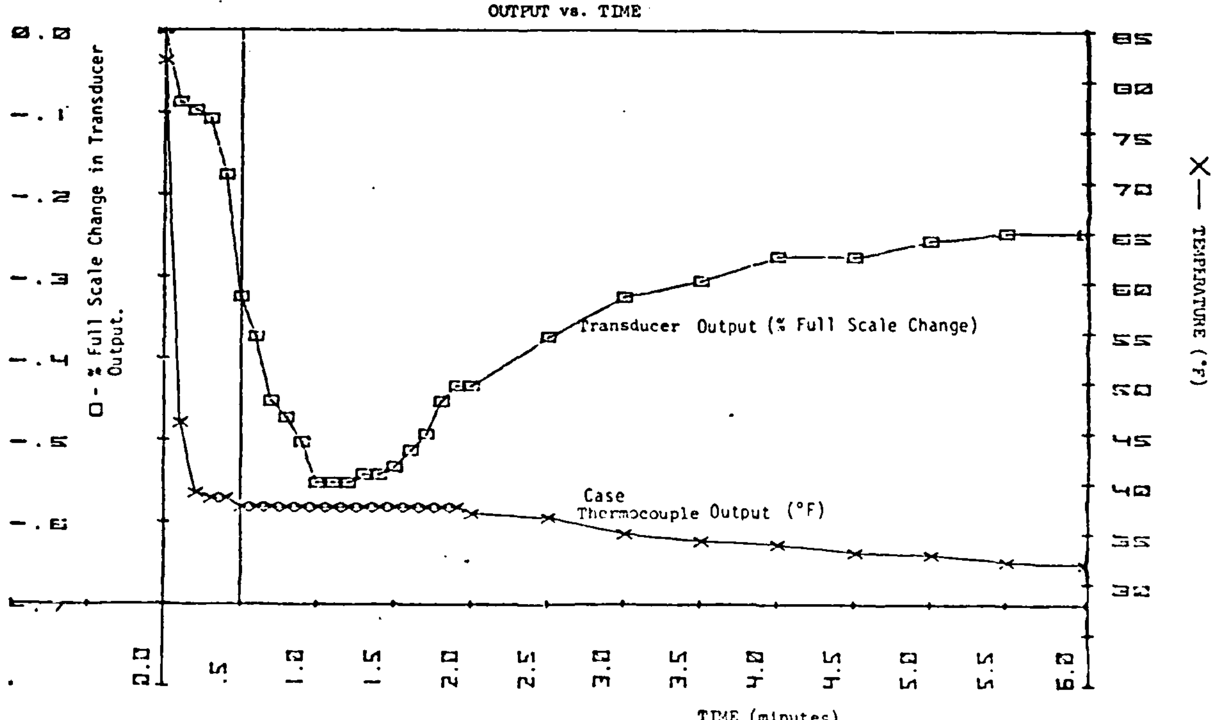

FIGURE 18

Pressure Step Response Test

(Burst Diaph. method)

GOULD
An Electrical/Electronics Company

MODEL: PA8223-60 S/N: 8049 DATE: 03-03-81 BY: MM/BT

UNIT ASSEM: 64884-500-600 (2215a) DIA/FLEXURE: 64876-000-130 "T" DIM: ______

BEAM: 64852-500-100 GAGE #: ______ SPECIAL WIRING: ______

EXCITATION VOLTAGE: 15 VDC INPUT RESISTANCE: 9662.3 Ω OUTPUT RESISTANCE: 5035.5 Ω

FULL SCALE = 50.376 mV/ 15 V/ 60 psia (open ckt)

TRUE RANGE: ______ psi NATURAL FREQUENCY: ______ Hz

Photo #1

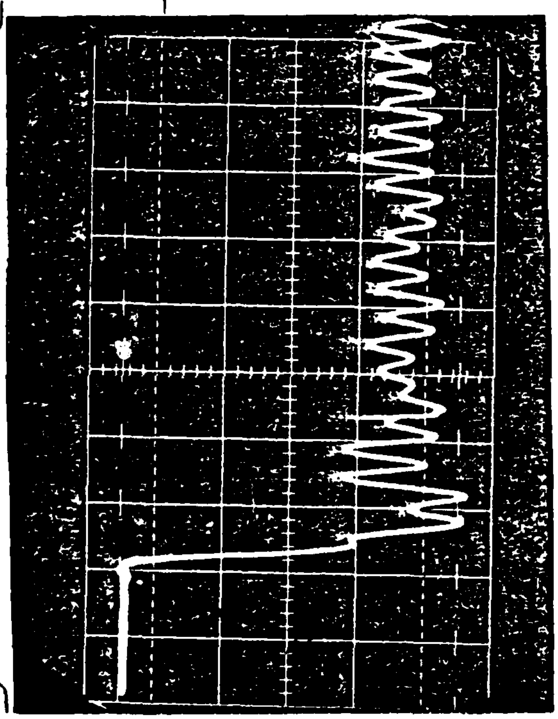

sweeptime (0.5 msec/cm)

pressure amplitude (10 psig/cm)

Photo #2

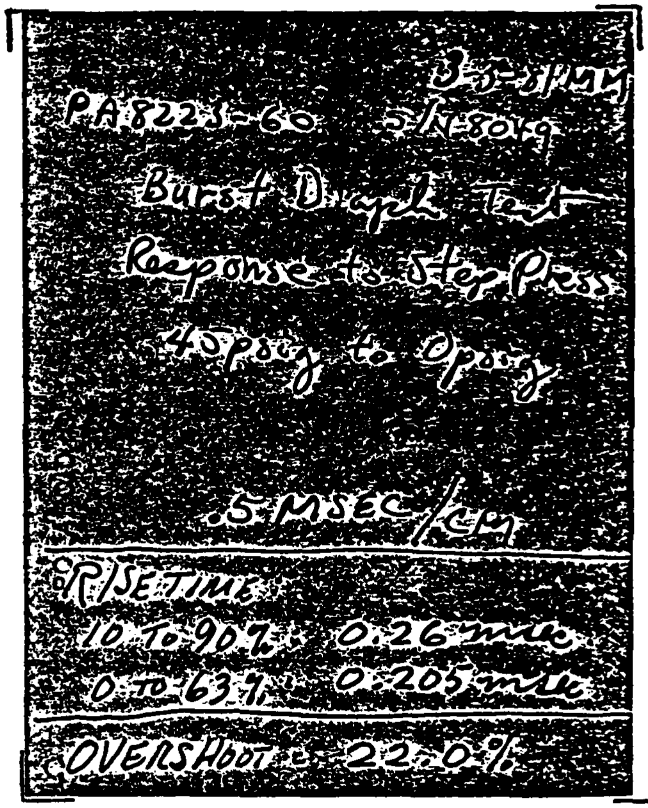

Pressure Step:
~~XXXXXXXXXXXXXXXXXX~~ 45 to 0 psig ~~psIX~~

Risetime:
~~XXXXXX~~: 10 to 90% = 0.26 msec ~~XXXXXX~~
0 to 63% = 0.205 msec

Pressure Chamber: ______ psi

OVERSHOOT = ~~Shock Pressure~~: 22.0 % ~~psi~~

Scope Horiz. Sweeptime: 0.5 msec/cm

Scope Vert. Sens: ______ mV/Div

Expansion Chamber: ______ psi

System: ______ filled

Pressure Chamber: ______ psi

Shock Pressure: ______ psi

Scope Horiz. Sweeptime: ______

Scope Vert. Sens: ______ mV/Div

Connecting Tube: ______

Connecting Fixtures: ______

Special Comments: ______

FIGURE 19

FIGURE 20

Pressure Step Response Test

(Burst Diaph. method)

GOULD
An Electrical/Electronics Company

MODEL: PA8223-20 S/N: 4446 DATE: 03-03-81 BY: MM/BT

UNIT ASSEM: 64885-500-200 (2214a) DIA/FLEXURE: 64878-000-050 "T" DIM: ______

BEAM: 64852-500-100 GAGE #: ______ SPECIAL WIRING: ______

EXCITATION VOLTAGE: 15 INPUT RESISTANCE: 5891.0 Ω OUTPUT RESISTANCE: 5084.9

FULL SCALE = 50.506 mV/ 15 V/ 20 psia (open ckt)

TRUE RANGE: ______ psi NATURAL FREQUENCY: ______ Hz

Photo #1	Photo #2

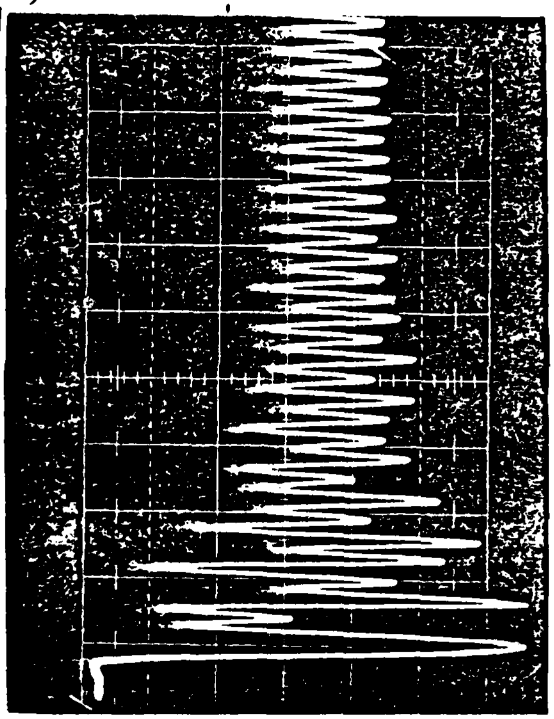

sweeptime (1.0 msec/cm)

pressure amplitude (1 psig/cm)

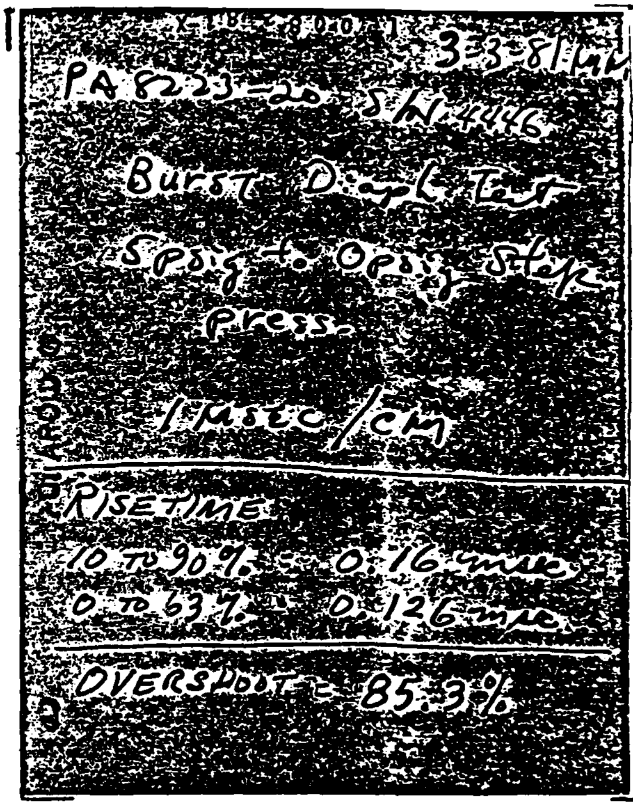

Pressure Step: ~~Expansion Chamber:~~ 5 to 0 psig ~~psi~~	Expansion Chamber: ______ psi
Risetime: ~~System:~~ 10 to 90% = 0.16 msec ~~filled~~ 0 to 63% = 0.126 msec	System: ______ filled
Pressure Chamber: ______ psi	Pressure Chamber: ______ psi
OVERSHOOT = ~~Shock Pressure:~~ 85.3% ~~psi~~	Shock Pressure: ______ psi
Scope Horiz. Sweeptime: 1.0 msec/~~XX~~cm	Scope Horiz. Sweeptime: ______
Scope Vert. Sens: ______ mV/Div	Scope Vert. Sens: ______ mV/Div

Connecting Tube: ______

Connecting Fixtures: ______

Special Comments: ______

FIGURE 20

DATE: 01-15-81

MODEL: PA8223-60

SERIAL: 8020

Basic Performance Tests

Excitation: 15 VDC

AS SHIPPED

PRESSURE (psia)	OUTPUT: MILLIVOLTS DC (OPEN CIRCUIT)					
	-65°F	-40°F	75°F	75°F	210°F	250°F
0	-0.340	-0.292	-0.176	-0.178	-0.282	-0.365
3	2.187	2.231	2.336	2.338	2.250	2.168
6	4.716	4.759	4.862	4.861	4.782	4.700
12	9.760	9.818	9.917	9.916	9.839	9.758
24	19.893	19.927	20.017	20.018	19.942	19.863
36	30.011	30.033	30.114	30.115	30.040	29.963
45	40.095	40.110	40.165	40.165	40.111	40.035
60	50.133	50.150	50.220	50.220	50.148	50.074
45	40.112	40.129	40.200	40.200	40.122	40.045
36	30.034	30.058	30.136	30.136	30.058	29.980
24	19.923	19.951	20.040	20.042	19.960	19.881
12	9.790	9.836	9.932	9.931	9.849	9.769
6	4.729	4.769	4.872	4.871	4.787	4.703
3	2.194	2.238	2.346	2.346	2.250	2.168
0	-0.339	-0.292	-0.178	-0.178	-0.282	-0.367
FULL SCALE SENSITIVITY(mV)	50.473	50.442	50.396	50.398	50.430	50.439
NON-LINEARITY ERROR (%FS)	+0.179	+0.168	+0.148	+0.149	+0.163	+0.162
HYSTERESIS ERROR (%FS)	+0.050	+0.050	+0.046	+0.048	+0.036	+0.036
REPEATABILITY ERROR (%FS)	X	X	X	+0.004	X	X
THERMAL SPAN ERROR (%/°F)	-0.0011	-0.0008	X	X	+0.0005	+0.0005
THERMAL ZERO ERROR (%FS/°F)	+0.0023	+0.0020	X	X	-0.0016	-0.0021

DATE: 06-18-82

MODEL: PA8223-60

SERIAL: 8020

Basic Performance Tests

Excitation: 15 VDC

AS RETURNED & RE-CALIBRATED

PRESSURE (psia)	OUTPUT: MILLIVOLTS DC (OPEN CIRCUIT)					
	-65°F	-40°F	75°F	75°F	210°F	250°F
0	-0.362	-0.307	-0.192	-0.188	-0.141	-0.272
3	2.173	2.225	2.341	2.343	2.391	2.202
6	4.708	4.761	4.875	4.876	4.923	4.797
12	9.775	9.828	9.937	9.937	9.984	9.860
24	19.903	19.946	20.050	20.045	20.093	19.976
36	30.022	30.065	30.158	30.149	30.230	30.055
45	40.111	40.155	40.241	40.227	40.274	40.165
60	50.175	50.205	50.294	50.273	50.317	50.216
45	40.150	40.167	40.257	40.240	40.236	40.160
36	30.063	30.091	30.183	30.170	30.216	30.104
24	19.941	19.975	20.076	20.067	20.114	19.995
12	9.805	9.851	9.956	9.953	9.980	9.873
6	4.731	4.777	4.887	4.885	4.931	4.802
3	2.193	2.239	2.349	2.349	2.344	2.204
0	-0.346	-0.300	-0.188	-0.187	-0.143	-0.276
FULL SCALE SENSITIVITY(mV)	50.537	50.512	50.486	50.461	50.458	[illegible]
NON-LINEARITY ERROR (%FS)	+0.203	+0.180	+0.165	+0.161	+0.183	+0.182
HYSTERESIS ERROR (%FS)	+0.061	+0.053	+0.051	+0.044	+0.042	+0.038
REPEATABILITY ERROR (%FS)	X	X	X	-0.042	X	X
THERMAL SPAN ERROR (%/°F)	-0.0007	-0.0004	X	X	-0.0004	±0.0000
THERMAL ZERO ERROR (%FS/°F)	+0.0024	+0.0020	X	X	+0.0007	-0.0009

FIGURE 21(A)

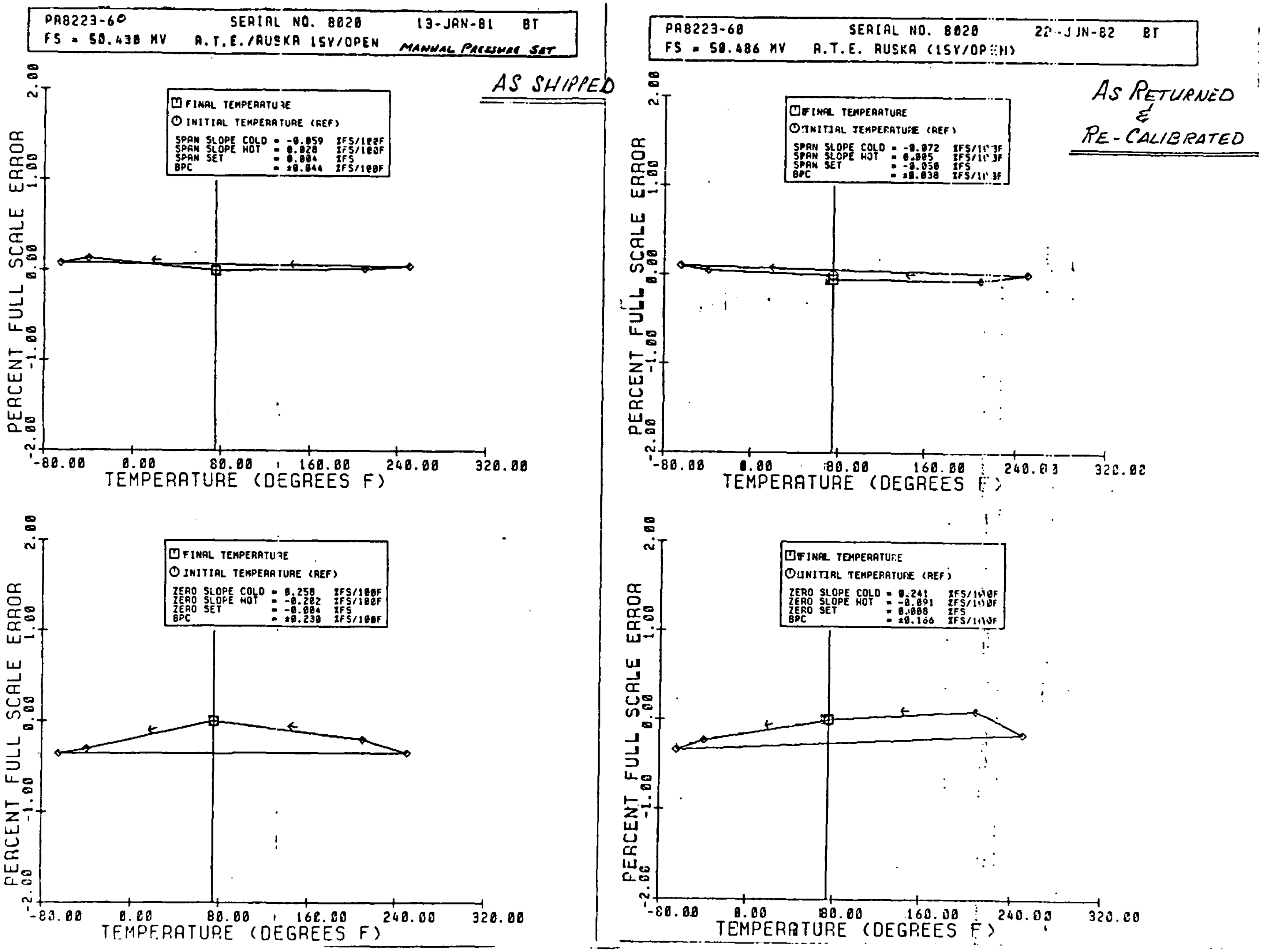
PA8223-6© SERIAL NO. 8020 13-JAN-81 BT
FS = 50.430 MV A.T.E./RUSKA 15V/OPEN MANUAL PRESSURE SET
AS SHIPPED
FINAL TEMPERATURE
INITIAL TEMPERATURE (REF)
SPAN SLOPE COLD = -0.059 %FS/100F
SPAN SLOPE HOT = 0.028 %FS/100F
SPAN SET = 0.004 %FS
BPC = ±0.044 %FS/100F
ZERO SLOPE COLD = 0.250 %FS/100F
ZERO SLOPE HOT = -0.202 %FS/100F
ZERO SET = -0.004 %FS
BPC = ±0.230 %FS/100F
PA8223-60 SERIAL NO. 8020 22-JUN-82 BT
FS = 50.486 MV A.T.E. RUSKA (15V/OPEN)
AS RETURNED & RE-CALIBRATED
SPAN SLOPE COLD = -0.072 %FS/100F
SPAN SLOPE HOT = 0.005 %FS/100F
SPAN SET = -0.050 %FS
BPC = ±0.038 %FS/100F
ZERO SLOPE COLD = 0.241 %FS/100F
ZERO SLOPE HOT = -0.091 %FS/100F
ZERO SET = 0.008 %FS
BPC = ±0.166 %FS/100F
PERCENT FULL SCALE ERROR
TEMPERATURE (DEGREES F)
-80.00 0.00 80.00 160.00 240.00 320.00
-2.00 -1.00 0.00 1.00 2.00

FIGURE 21(B)

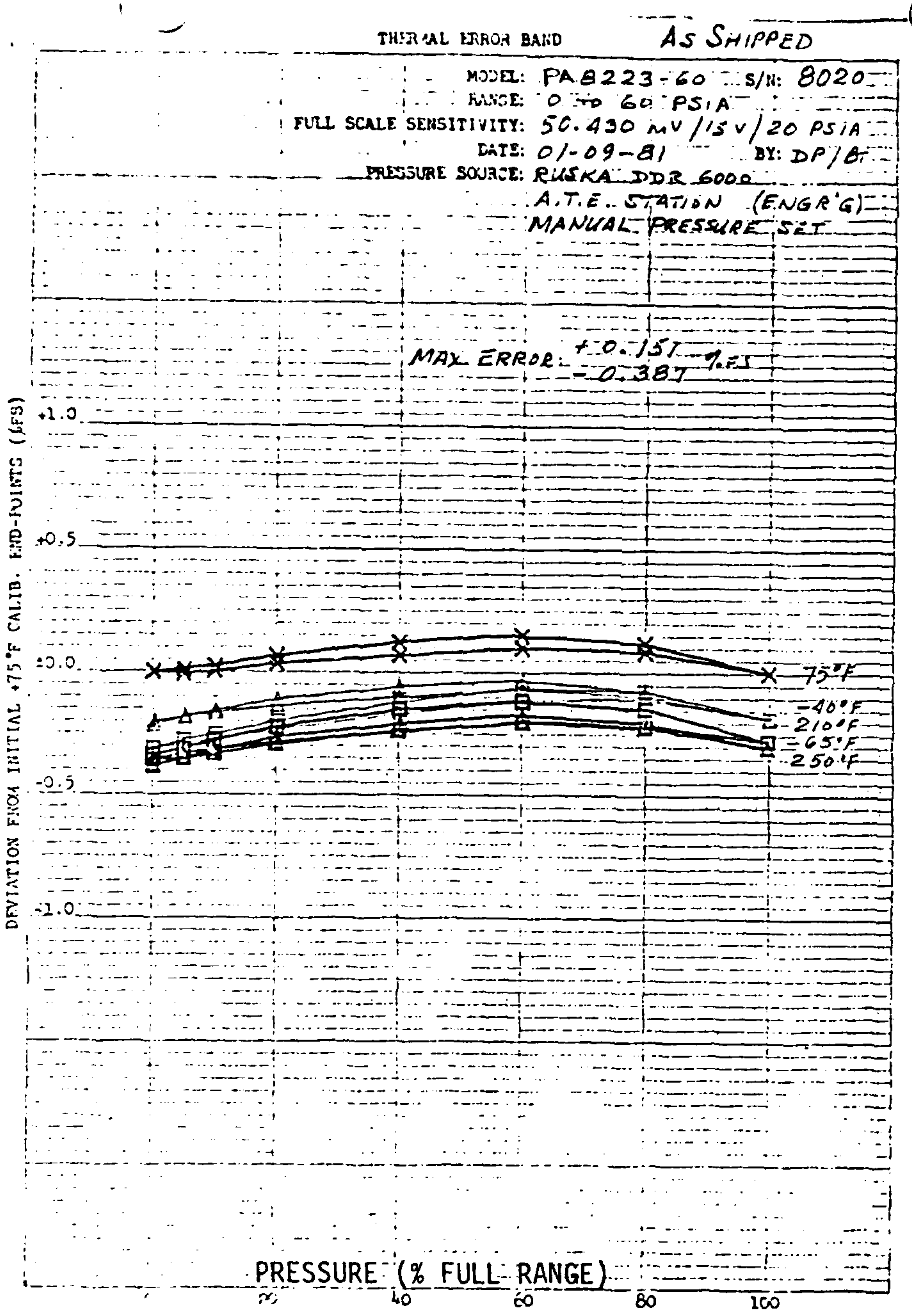
THERMAL ERROR BAND
As Shipped
MODEL: PA8223-60 S/N: 8020
RANGE: 0 to 60 PSIA
FULL SCALE SENSITIVITY: 50.430 MV/15V/20 PSIA
DATE: 01-09-81 BY: DP/B
PRESSURE SOURCE: RUSKA DDR 6000
A.T.E. STATION (ENGR'G)
MANUAL PRESSURE SET
MAX ERROR: +0.151 -0.387 %FS
75°F
-40°F
210°F
-65°F
250°F
DEVIATION FROM INITIAL +75°F CALIB. END-POINTS (%FS)
PRESSURE (% FULL RANGE)

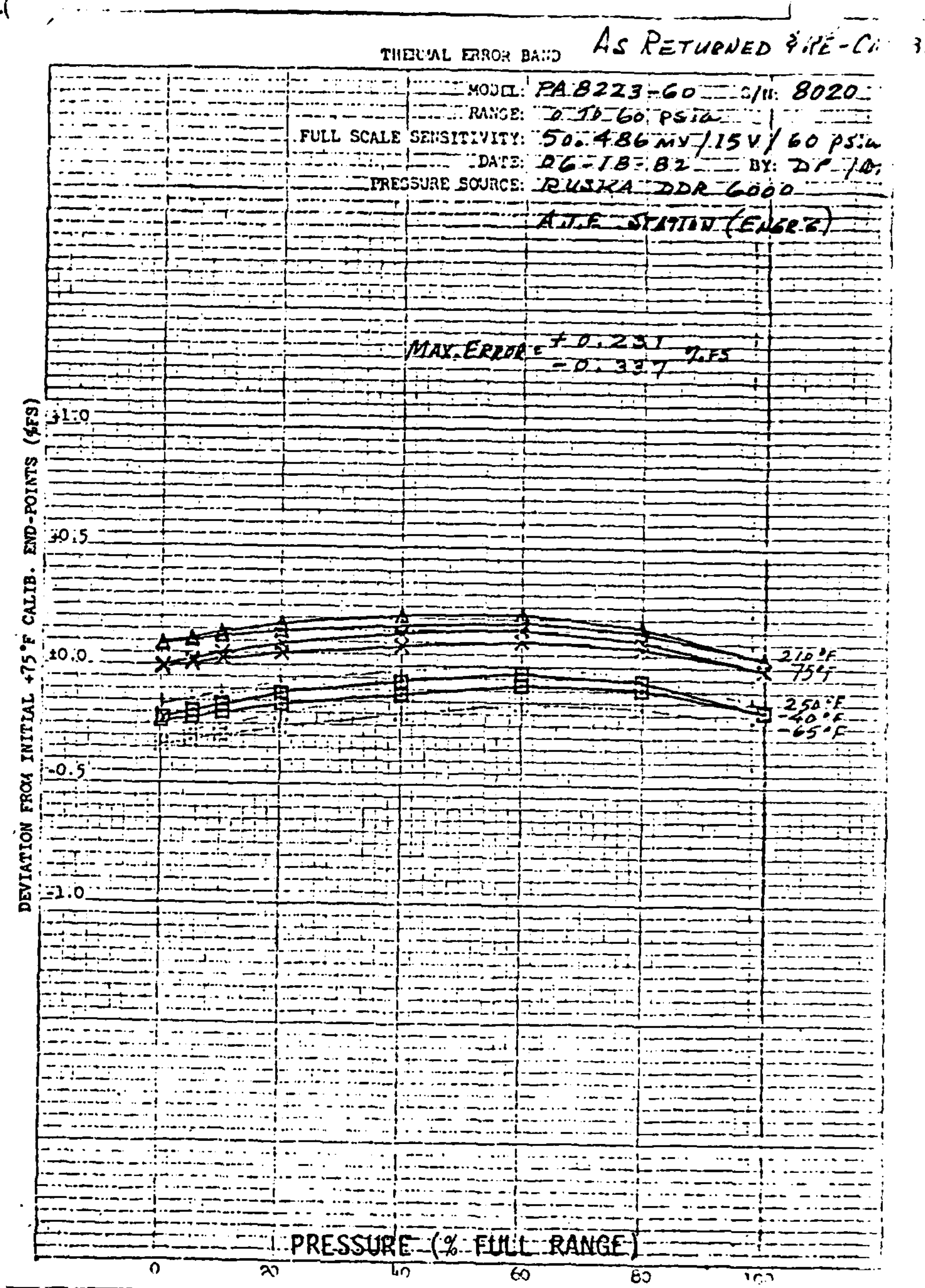
THERMAL ERROR BAND
As Returned
MODEL: PA8223-60 S/N: 8020
RANGE: 0 to 60 PSIA
FULL SCALE SENSITIVITY: 50.486 MV/15V/60 PSIA
DATE: 06-18-82
PRESSURE SOURCE: RUSKA DDR 6000
A.T.E. STATION (ENGR'G)
MAX. ERROR = +0.231 -0.327 %FS
210°F
75°F
250°F
-40°F
-65°F
DEVIATION FROM INITIAL +75°F CALIB. END-POINTS (%FS)
PRESSURE (% FULL RANGE)

FIGURE 21(C)

DATE: 01-15-81
MODEL: PA8223-20
SERIAL: 4387
Basic Performance Tests
Excitation: 15 VDC

AS SHIPPED

PRESSURE (psia)	OUTPUT: MILLIVOLTS DC (OPEN CIRCUIT)					
	-65°F	-40°F	75°F	75°F	210°F	250°F
0	-0.294	-0.258	-0.101	-0.100	-0.125	-0.225
1	2.220	2.257	2.412	2.413	2.391	2.291
2	4.737	4.771	4.927	4.929	4.806	4.807
4	9.772	9.804	9.962	9.961	9.941	9.845
8	19.855	19.880	20.041	20.041	20.025	19.934
12	29.940	29.965	30.127	30.126	30.119	30.030
16	40.043	40.058	40.220	40.220	40.218	40.132
20	50.148	50.151	50.317	50.318	50.321	50.236
16	40.059	40.071	40.242	40.234	40.227	40.142
12	29.960	29.985	30.147	30.147	30.131	30.045
8	19.876	19.900	20.059	20.059	20.037	19.946
4	9.757	9.818	9.975	9.975	9.945	9.852
2	4.747	4.781	4.937	4.936	4.903	4.809
1	2.228	2.264	2.418	2.419	2.381	2.287
0	-0.294	-0.258	-0.099	-0.100	-0.129	-0.228
FULL SCALE SENSITIVITY (mV)	50.442	50.409	50.418	50.418	50.446	50.461
NON-LINEARITY ERROR (%FS)	-0.055	-0.051	-0.050	-0.052	-0.056	-0.050
HYSTERESIS ERROR (%FS)	+0.042	+0.040	+0.044	+0.042	+0.024	+0.030
REPEATABILITY ERROR (%FS)				-0.016		
THERMAL SPAN ERROR (%/°F)	-0.0012	+0.0002			+0.0004	+0.0005
THERMAL ZERO ERROR (%FS/°F)	+0.0027	+0.0027			-0.0004	-0.001

DATE: 06-15-82
MODEL: PA8223-20
SERIAL: 4387
Basic Performance Tests
Excitation: 15 VDC

AS RETURNED & RE-CALIBRATED

PRESSURE (psia)	OUTPUT: MILLIVOLTS DC (OPEN CIRCUIT)					
	-65°F	-40°F	75°F	75°F	210°F	250°F
0	-0.277	-0.238	-0.034	-0.034	0.055	[illegible]
1	2.246	2.279	2.478	2.480	2.573	[illegible]
2	4.766	4.796	4.995	4.997	5.081	[illegible]
4	9.805	9.833	10.032	10.034	10.130	[illegible]
8	19.894	19.919	20.118	20.119	20.222	[illegible]
12	29.992	30.013	30.210	30.213	30.321	[illegible]
16	40.094	40.111	40.311	40.313	40.426	[illegible]
20	50.200	50.217	50.414	50.416	50.535	[illegible]
16	40.114	40.129	40.324	40.325	40.441	[illegible]
12	30.021	30.036	30.230	30.230	30.335	[illegible]
8	19.927	19.945	20.137	20.137	20.240	[illegible]
4	9.835	9.855	10.047	10.047	10.143	[illegible]
2	4.792	4.816	5.005	5.005	5.097	[illegible]
1	2.273	2.296	2.485	2.485	2.573	[illegible]
0	-0.240	-0.224	-0.034	-0.034	0.055	[illegible]
FULL SCALE SENSITIVITY (mV)	50.477	50.455	50.448	50.450	[illegible]	[illegible]
NON-LINEARITY ERROR (%FS)	+0.061	-0.050	-0.054	[illegible]	[illegible]	[illegible]
HYSTERESIS ERROR (%FS)	+0.065	+0.032	+0.040	+0.035	+0.030	[illegible]
REPEATABILITY ERROR (%FS)				+0.036		
THERMAL SPAN ERROR (%/°F)	-0.0004	-0.0001			+0.0005	[illegible]
THERMAL ZERO ERROR (%FS/°F)	+0.0034	+0.0035			+0.0013	[illegible]

FIGURE 22(A)

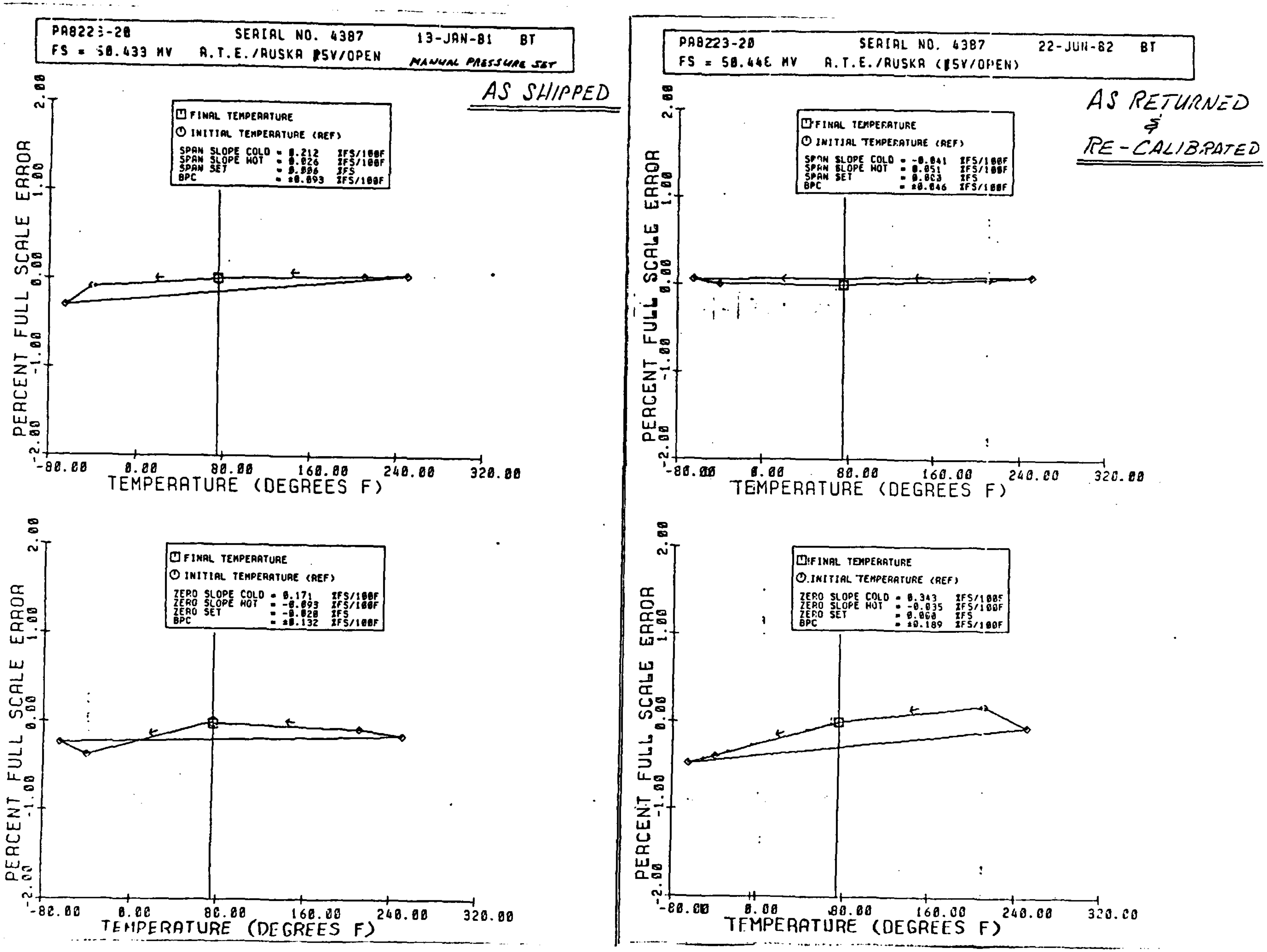
PA8223-20 SERIAL NO. 4387 13-JAN-81 BT
FS = 50.433 MV A.T.E./RUSKA 5V/OPEN MANUAL PRESSURE SET
AS SHIPPED
FINAL TEMPERATURE
INITIAL TEMPERATURE (REF)
SPAN SLOPE COLD = 0.212 %FS/100F
SPAN SLOPE HOT = 0.026 %FS/100F
SPAN SET = 0.006 %FS
BPC = ±0.093 %FS/100F
ZERO SLOPE COLD = 0.171 %FS/100F
ZERO SLOPE HOT = -0.093 %FS/100F
ZERO SET = -0.020 %FS
BPC = ±0.132 %FS/100F
PA8223-20 SERIAL NO. 4387 22-JUN-82 BT
FS = 50.446 MV A.T.E./RUSKA (5V/OPEN)
AS RETURNED & RE-CALIBRATED
SPAN SLOPE COLD = -0.041 %FS/100F
SPAN SLOPE HOT = 0.051 %FS/100F
SPAN SET = 0.003 %FS
BPC = ±0.046 %FS/100F
ZERO SLOPE COLD = 0.343 %FS/100F
ZERO SLOPE HOT = -0.035 %FS/100F
ZERO SET = 0.060 %FS
BPC = ±0.189 %FS/100F
PERCENT FULL SCALE ERROR
TEMPERATURE (DEGREES F)
-80.00 0.00 80.00 160.00 240.00 320.00
-2.00 -1.00 0.00 1.00 2.00

FIGURE 22(B)

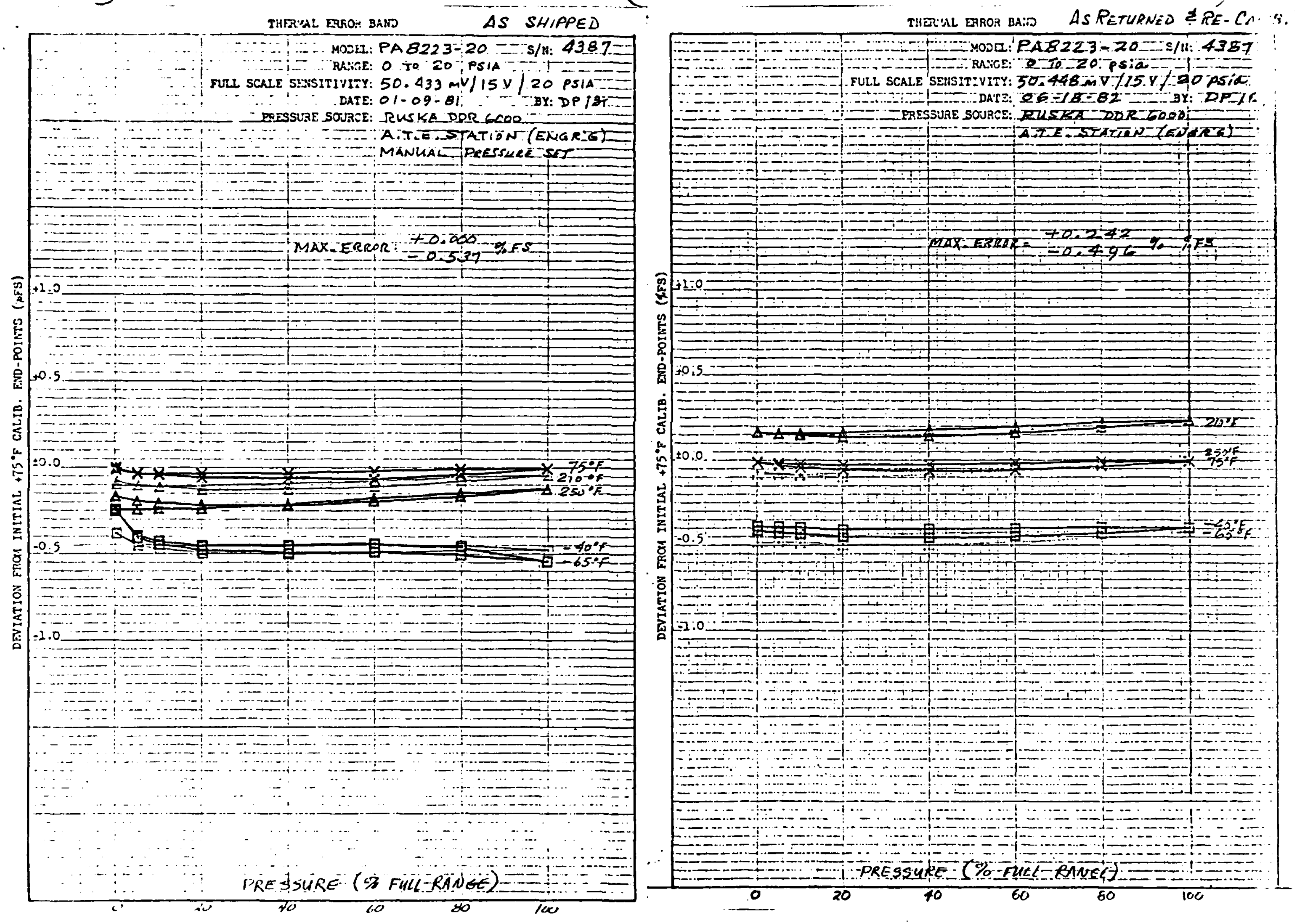
THERMAL ERROR BAND AS SHIPPED
MODEL: PA8223-20 S/N: 4387
RANGE: 0 TO 20 PSIA
FULL SCALE SENSITIVITY: 50.433 mV/15V/20 PSIA
DATE: 01-09-81 BY: DP
PRESSURE SOURCE: RUSKA DDR 6000
A.T.E. STATION (ENGR'G)
MANUAL PRESSURE SET
MAX. ERROR: +0.000 -0.537 % FS
DEVIATION FROM INITIAL +75°F CALIB. END-POINTS (%FS)
+1.0
+0.5
±0.0
-0.5
-1.0
75°F
210°F
250°F
-40°F
-65°F
PRESSURE (% FULL RANGE)
20
40
60
80
100
THERMAL ERROR BAND AS RETURNED & RE-CAL'D.
MODEL: PA8223-20 S/N: 4387
RANGE: 0 TO 20 psia
FULL SCALE SENSITIVITY: 50.448 mV/15V/20 psia
DATE: 06-18-82 BY: DP
PRESSURE SOURCE: RUSKA DDR 6000
A.T.E. STATION (ENGR'G)
MAX. ERROR = +0.242 -0.496 % FS
DEVIATION FROM INITIAL +75°F CALIB. END-POINTS (%FS)
+1.0
+0.5
±0.0
-0.5
-1.0
210°F
250°F
75°F
-40°F
-65°F
PRESSURE (% FULL RANGE)
0
20
40
60
80
100

FIGURE 22(C)

TABLES

MODEL: PA8223-20

SERIAL: 4387

Basic Performance Tests

Excitation: 15 VDC

TABLE 1

PROTOTYPE INITIAL DESIGN VALIDATION TEST RESULTS

INPUT RESISTANCE 5611.3 ohms

OUTPUT RESISTANCE 4819.2 ohms

INSULATION RESISTANCE (MEGOHM at 50 VDC) 100 K

CALIBRATION FACTOR (OPEN CIRCUIT) 168.06 μV/V/psi

PRESSURE (psia)	OUTPUT: MILLIVOLTS DC (OPEN CIRCUIT)					
	-65°F	-40°F	75°F	75°F	210°F	250°F
0	-0.294	-0.258	-0.101	-0.100	-0.125	-0.225
1	2.220	2.257	2.412	2.413	2.391	2.291
2	4.737	4.771	4.927	4.929	4.806	4.807
4	9.772	9.804	9.962	9.961	9.941	9.845
8	19.855	19.880	20.041	20.041	20.025	19.934
12	29.946	29.965	30.127	30.126	30.119	30.030
16	40.043	40.058	40.220	40.220	40.218	40.132
20	50.148	50.151	50.317	50.318	50.321	50.236
16	40.059	40.071	40.242	40.234	40.227	40.142
12	29.966	29.985	30.147	30.147	30.131	30.045
8	19.876	19.900	20.059	20.059	20.037	19.946
4	9.787	9.818	9.975	9.975	9.945	9.852
2	4.747	4.781	4.937	4.936	4.903	4.809
1	2.228	2.264	2.418	2.419	2.381	2.287
0	-0.294	-0.258	-0.099	-0.100	-0.129	-0.228
FULL SCALE SENSITIVITY (mV)	50.442	50.409	50.418	50.418	50.446	50.461
NON-LINEARITY ERROR (%FS)	-0.055	-0.051	-0.050	-0.052	-0.056	-0.050
HYSTERESIS ERROR (%FS)	+0.042	+0.040	+0.044	+0.042	+0.024	+0.030
REPEATABILITY ERROR (%FS)	X	X	X	-0.016	X	X
THERMAL SPAN ERROR (%/°F)	-0.0012	+0.0002	X	X	+0.0004	+0.0005
THERMAL ZERO ERROR (%FS/°F)	+0.0027	+0.0027	X	X	-0.0004	-0.0014

DATE: 01-15-81

MODEL: PA8223-60

SERIAL: 8020

Basic Performance Tests

Excitation: 15 VDC

TABLE 2

PROTOTYPE INITIAL DESIGN VALIDATION TEST RESULTS

INPUT RESISTANCE 9562.0 ohms

OUTPUT RESISTANCE 5111.9 ohms

INSULATION RESISTANCE (MEGOHMS at 50 VDC) 15K

CALIBRATION FACTOR (OPEN CIRCUIT) 55.996 μV/V/psi

PRESSURE (psia)	OUTPUT: MILLIVOLTS DC (OPEN CIRCUIT)					
	-65°F	-40°F	75°F	75°F	210°F	250°F
0	-0.340	-0.292	-0.176	-0.178	-0.282	-0.365
3	2.187	2.231	2.338	2.338	2.250	2.168
6	4.716	4.759	4.862	4.861	4.782	4.700
12	9.780	9.818	9.917	9.916	9.839	9.758
24	19.898	19.927	20.017	20.018	19.942	19.863
36	30.011	30.033	30.114	30.115	30.040	29.963
48	40.095	40.110	40.185	40.185	40.111	40.035
60	50.133	50.150	50.220	50.220	50.148	50.074
48	40.112	40.129	40.200	40.200	40.122	40.045
36	30.034	30.058	30.136	30.136	30.058	29.980
24	19.923	19.951	20.040	20.042	19.960	19.881
12	9.798	9.836	9.932	9.931	9.849	9.769
6	4.729	4.769	4.872	4.871	4.787	4.703
3	2.194	2.238	2.346	2.346	2.250	2.168
0	-0.339	-0.292	-0.178	-0.178	-0.282	-0.367
FULL SCALE SENSITIVITY (mV)	50.473	50.442	50.396	50.398	50.430	50.439
NON-LINEARITY ERROR (%FS)	+0.179	+0.168	-0.148	+0.149	+0.163	+0.162
HYSTERESIS ERROR (%FS)	+0.050	+0.050	+0.046	+0.048	+0.036	+0.036
REPEATABILITY ERROR (%FS)	X	X	X	+0.004	X	X
THERMAL SPAN ERROR (%/°F)	-0.0011	-0.0008	X	X	+0.0005	+0.0005
THERMAL ZERO ERROR (%FS/°F)	+0.0023	+0.0020	X	X	-0.0016	-0.0021

DATE: 01-15-81

MODEL: PA 8223-20

SERIAL: 4446

Basic Performance Tests

Excitation: 15 VDC

TABLE 3

PROTOTYPE INITIAL DESIGN VALIDATION TEST RESULTS

INPUT RESISTANCE 5891.0 ohms

OUTPUT RESISTANCE 5084.9 ohms

INSULATION RESISTANCE (MEGOHMS at 50 VDC) 25K

CALIBRATION FACTOR (OPEN CIRCUIT) 168.353 μV/V/psi

PRESSURE (psia)	OUTPUT: MILLIVOLTS DC (OPEN CIRCUIT)					
	-65°F	-40°F	75°F	75°F	210°F	250°F
0	-0.170	-0.164	-0.023	-0.024	-0.074	-0.176
1	2.356	2.361	2.500	2.498	2.447	2.343
2	4.883	4.885	5.023	5.023	4.965	4.860
4	9.938	9.938	10.072	10.070	10.007	9.901
8	20.058	20.081	20.177	20.176	20.101	19.991
12	30.174	30.162	30.284	30.281	30.200	30.087
16	40.285	40.265	40.387	40.383	40.299	40.183
20	50.393	50.362	50.483	50.482	50.389	50.272
16	40.303	40.281	40.411	40.403	40.309	40.194
12	30.199	30.186	30.308	30.306	30.212	30.102
8	20.084	20.075	20.199	20.198	20.112	20.006
4	9.957	9.955	10.086	10.084	10.011	9.909
2	4.895	4.897	5.033	5.031	4.963	4.863
1	2.364	2.367	2.506	2.504	2.438	2.339
0	-0.170	-0.163	-0.021	-0.023	-0.078	-0.178
FULL SCALE SENSITIVITY (mV)	50.563	50.526	50.506	50.506	50.463	50.448
NON-LINEARITY ERROR (%FS)	+0.062	+0.068	+0.058	+0.052	+0.025	-0.025
HYSTERESIS ERROR (%FS)	+0.051	+0.048	+0.048	+0.049	+0.024	+0.030
REPEATABILITY ERROR (%FS)	X	X	X	-0.016	X	X
THERMAL SPAN ERROR (%/°F)	-0.0008	-0.0003	X	X	-0.0006	-0.0007
THERMAL ZERO ERROR (%FS/°F)	+0.0021	+0.0024	X	X	-0.0007	-0.0017

DATE : 01-15-81

MODEL: PA 8223-60

SERIAL: 8049

Basic Performance Tests

Excitation: 15 VDC

TABLE 4

PROTOTYPE INITIAL DESIGN VALIDATION TEST RESULTS

INPUT RESISTANCE 9662.3 ohms

OUTPUT RESISTANCE 5035.5 ohms

INSULATION RESISTANCE (MEGOHM at 50 VDC) 74 K

CALIBRATION FACTOR (OPEN CIRCUIT) 55.973 μV/V/psi

PRESSURE (psia)	OUTPUT: MILLIVOLTS DC (OPEN CIRCUIT)					
	-65°F	-40°F	75°F	75°F	210°F	250°F
0	-0.376	-0.328	-0.230	-0.232	-0.308	-0.398
3	2.158	2.203	2.298	2.296	2.222	2.130
6	4.692	4.735	4.828	4.826	4.752	4.661
12	9.762	9.799	9.887	9.884	9.812	9.723
24	19.865	19.892	19.978	19.977	19.921	19.836
36	29.953	29.972	30.052	30.050	30.003	29.923
48	40.024	40.036	40.107	40.105	40.060	39.982
60	50.078	50.085	50.146	50.144	50.097	50.022
48	40.038	40.052	40.121	40.120	40.070	39.992
36	29.975	29.994	30.073	30.071	30.021	29.939
24	19.888	19.915	20.001	19.999	19.937	19.852
12	9.777	9.814	9.901	9.898	9.821	9.731
6	4.702	4.743	4.835	4.833	4.754	4.662
3	2.163	2.207	2.303	2.300	2.220	2.129
0	-0.376	-0.328	-0.230	-0.232	-0.308	-0.399
FULL SCALE SENSITIVITY (mV)	50.454	50.413	50.376	50.376	50.405	50.420
NON-LINEARITY ERROR (%FS)	+0.163	+0.154	+0.160	+0.160	+0.171	+0.169
HYSTERESIS ERROR (%FS)	+0.046	+0.046	+0.046	+0.044	+0.036	+0.032
REPEATABILITY ERROR (%FS)	X	X	X	-0.006	X	X
THERMAL SPAN ERROR (%/°F)	-0.0011	-0.0006	X	X	+0.0004	+0.0005
THERMAL ZERO ERROR (%FS/°F)	+0.0021	+0.0017	X	X	-0.0011	-0.0019

TABLE 5

DATE: [illegible]
MODEL: [illegible]
SERIAL: [illegible]

Excitation: 15 V DC

BASIC PERFORMANCE TEST - INITIAL STATIC ACCURACY

COLUMN #	1	2	3	4	5	6
PRESSURE (psia) Ruska ±.[illegible]	OUTPUT: MILLIVOLTS DC -65°F	-40°F	75°F	75°F	210°F	250°F
0	-.153	-.180	.010	.010	.039	-.086
1	2.369	2.343	2.532	2.533	2.557	2.429
2	4.895	4.869	5.056	5.056	5.076	4.947
4	9.951	9.923	10.106	10.105	10.117	9.988
8	20.070	20.041	20.211	20.210	20.212	20.079
12	30.186	30.158	30.317	30.317	30.311	30.179
16	40.293	40.265	40.423	40.422	40.410	40.277
20	50.400	50.367	50.522	50.522	50.502	50.372
16	40.311	40.281	40.438	40.437	40.420	40.289
12	30.211	30.181	30.340	30.339	30.324	30.192
8	20.095	20.064	20.230	20.230	20.223	20.094
4	9.970	9.940	10.119	10.118	10.123	9.995
2	4.909	4.880	5.064	5.063	5.075	4.951
1	2.379	2.349	2.537	2.536	2.554	2.428
0	-.154	-.180	.010	.010	.038	-.086
FULL SCALE SENSITIVITY (mV)	50.553	50.547	50.512	50.512	50.463	50.458
NON-LINEARITY ERROR (% FS)	+0.064	+0.065	+0.045	+0.043	-0.029	-0.036
HYSTERESIS ERROR (% FS)	+0.049	+0.046	+0.046	+0.044	+0.026	+0.030
REPEATABILITY ERROR (% FS)				±0.002		
THERMAL SPAN ERROR (%/°F)	-0.0006	-0.0006			-0.0007	-0.0006
THERMAL ZERO ERROR (% FS/°F)	+0.0023	-.0033			+0.0004	-0.0011

STATIC CALIBRATION TEST DATA AFTER PROGRESSIVE ENVIRONMENTAL TESTS

RUSKA PRESSURE (psia)	7	8	9	10	11	12	13
	OUTPUT: MILLIVOLTS DC STATIC ACCURACY TESTS: 75°F						
0	-.040	-.012	-.040	-.001	-.016	-.009	-.003
1	2.496	2.525	2.478	2.537	2.505	2.523	2.523
2	5.020	5.050	5.004	5.062	5.029	5.049	5.049
4	10.070	10.099	10.056	10.114	10.083	10.100	10.102
8	20.180	20.212	20.169	20.227	20.197	20.214	20.217
12	30.289	30.323	30.278	30.346	30.312	30.332	30.333
16	40.392	40.426	40.382	40.457	40.423	40.449	40.449
20	50.492	50.528	50.483	50.567	50.530	50.557	50.554
16	40.406	40.442	40.398	40.470	40.438	40.461	40.458
12	30.308	30.341	30.298	30.362	30.332	30.353	30.351
8	20.198	20.229	20.188	20.248	20.217	20.236	20.236
4	10.082	10.113	10.073	10.128	10.097	10.117	10.117
2	5.026	5.056	5.014	5.069	5.041	5.057	5.058
1	2.497	2.528	2.488	2.541	2.514	2.530	2.532
0	-.040	-.012	-.040	-.001	-.015	-.009	-.003
FULL SCALE SENSITIVITY (mV)	50.532	50.540	50.523	50.568	50.546	50.566	50.557
NON-LINEARITY ERROR (% FS)	+0.057	+0.057	+0.048	+0.044	+0.040	+0.044	+0.039
HYSTERESIS ERROR (% FS)	+0.038	+0.036	+0.040	+0.042	+0.040	+0.044	+0.038
	Post Temperature Cycling Data	Post Static Acceleration Test	Post Shock Test	Post Sine Vibration	Post Humidity Test	Post Pressure Cycling Test	Post Thermal Shock Test

ACCURACY GOALS

Static Accuracy:	Thermal Effects:
Non-linearity, < ± .15% F.S. terminal	Compensated from -65 to +250°F
Hysteresis, < 0.1% F.S.	Zero Shift, < 0.005% F.S./°F
Repeatability:	Sensitivity Shift, < 0.005%/°F
Repeatability, < 0.1% F.S.	

TABLE 6

DATE: 03-04-81
MODEL: [illegible]
SERIAL: 5049

Excitation: 15 V DC

BASIC PERFORMANCE TESTS - INITIAL STATIC ACCURACY

COLUMN #	1	2	3	4	5	6
PRESSURE (psia) Ruska ±.050	OUTPUT: MILLIVOLTS DC -65°F	-40°F	75°F	75°F	210°F	250°F
0	-.351	-.336	-.210	-.210	-.228	-.340
3	2.192	2.195	2.318	2.319	2.305	2.189
6	4.716	4.727	4.848	4.848	4.834	4.721
12	9.783	9.794	9.908	9.908	9.894	9.782
24	19.840	19.901	20.007	20.006	20.004	19.896
36	29.930	29.987	30.082	30.083	30.086	29.985
48	40.053	40.058	40.140	40.140	40.142	40.046
60	50.112	50.114	50.181	50.181	50.182	50.091
48	-0.068	40.074	40.154	40.153	40.154	40.055
36	30.002	30.011	30.104	30.104	30.102	30.003
24	19.914	19.925	20.028	20.029	20.020	19.913
12	9.798	9.809	9.922	9.922	9.903	9.790
6	4.724	4.736	4.855	4.855	4.836	4.722
3	2.186	2.200	2.322	2.323	2.305	2.188
0	-.351	-.336	-.210	-.210	-.230	-.341
FULL SCALE SENSITIVITY (mV)	50.463	50.450	50.391	50.391	50.410	50.431
NON-LINEARITY ERROR (% FS)	+0.158	+0.161	+0.162	+0.164	+0.167	+0.167
HYSTERESIS ERROR (% FS)	+0.049	+0.048	+0.044	+0.046	+0.032	+0.036
REPEATABILITY ERROR (% FS)				±0.002		
THERMAL SPAN ERROR (%/°F)	-0.0010	-0.0010			+0.0003	+0.0005
THERMAL ZERO ERROR (% FS/°F)	+0.0020	+0.0022			-0.0003	-0.0015

STATIC CALIBRATION TEST DATA AFTER PROGRESSIVE ENVIRONMENTAL TESTS

COLUMN #	7	8	9	10	11	12	13
RUSKA PRESSURE (psia)	OUTPUT: MILLIVOLTS DC STATIC ACCURACY TESTS: 75°F						
0	-.476	-.467	-.490	-.476	-.480	-.465	-.464
3	2.059	2.066	2.040	2.058	2.048	2.065	2.067
6	4.590	4.596	4.572	4.589	4.581	4.597	4.599
12	9.653	9.660	9.636	9.654	9.644	9.661	9.663
24	19.755	19.761	19.741	19.758	19.749	19.776	19.780
36	29.834	29.840	29.822	29.840	29.828	29.863	29.868
48	39.892	39.898	39.880	39.897	39.886	39.921	39.926
60	49.934	49.940	49.923	49.937	49.931	49.961	49.968
48	39.904	39.910	39.892	39.910	39.899	39.932	39.938
36	29.854	29.860	29.841	29.860	29.848	29.882	29.886
24	19.775	19.781	19.761	19.778	19.769	19.794	19.798
12	9.666	9.673	9.650	9.667	9.659	9.673	9.676
6	4.598	4.604	4.580	4.598	4.589	4.604	4.606
3	2.062	2.069	2.045	2.062	2.053	2.068	2.070
0	-.476	-.467	-.490	-.476	-.479	-.465	-.464
FULL SCALE SENSITIVITY (mV)	50.410	50.407	50.413	50.413	50.411	50.426	50.432
NON-LINEARITY ERROR (% FS)	+0.173	+0.169	+0.170	+0.176	+0.168	+0.181	+0.180
HYSTERESIS ERROR (% FS)	+0.040	+0.040	+0.040	+0.040	+0.040	+0.038	+0.036
	Post Temperature Cycling Data	Post Static Acceleration Test	Post Shock Test	Post Sine Vibration	Post Humidity Test	Post Pressure Cycling Test	Post Thermal Shock Test

ACCURACY GOALS

Static Accuracy:	Thermal Effects:
Non-linearity, < ± .15% F.S. terminal	Compensated from -65 to +250°F
Hysteresis, < 0.1% F.S.	Zero Shift, < 0.005% F.S./°F
Repeatability:	Sensitivity Shift, < 0.005%/°F
Repeatability, < 0.1% F.S.	

:: 2-23-81

EL: PA8223-20

IAL: 4446

tic Acceleration Test Report

citation: 15 V DC Temperature: 79°F

10g Level for 5 Seconds

"G" evel	+X Axis mV	-X Axis mV	+Y Axis mV	-Y Axis mV	+Z Axis mV	-Z Axis mV
0	37.064	37.062	37.022	37.007	36.967	37.026
10	37.431	36.688	37.015	37.002	36.964	37.023
10	37.430	36.687	37.013	37.005	36.963	37.023
10	37.430	36.685	37.016	37.004	36.962	37.023
10	37.430	36.688	37.015	37.002	36.965	37.015
10	37.430	36.685	37.010	37.002	36.964	37.020
10	37.430	36.686	37.015	37.002	36.960	37.020
10	37.428	36.686	37.010	36.997	36.963	37.018
10	37.428	36.686	37.010	37.000	36.963	37.015
10	37.428	36.685	37.012	36.997	36.962	37.018
10	37.428	36.686	37.010	36.997	36.962	37.021
0	37.063	37.053	37.010	36.996	36.962	37.021

DATE: 2-23-81

MODEL: PA8223-60

SERIAL: 8049

Static Acceleration Test Report

Excitation: 15 V DC Temperature: 79°F

10g Level for 5 Seconds

"G" Level	+X Axis	-X Axis	+Y Axis	-Y Axis	+Z Axis	-Z Axis
0	11.896	11.895	11.893	11.891	11.888	11.885
10	12.010	11.775	11.893	11.890	11.890	11.882
10	12.010	11.775	11.894	11.890	11.890	11.882
10	12.010	11.777	11.894	11.890	11.885	11.883
10	12.010	11.775	11.895	11.890	11.886	11.882
10	12.010	11.775	11.893	11.890	11.885	11.882
10	12.010	11.776	11.894	11.890	11.895	11.881
10	12.010	11.776	11.895	11.890	11.885	11.880
10	12.010	11.776	11.892	11.890	11.887	11.880
10	12.010	11.777	11.890	11.890	11.885	11.880
10	12.010	11.776	11.890	11.890	11.882	11.881
0	11.895	11.895	11.890	11.890	11.887	11.883

TABLE 7

☆U.S.Government Printing Office: 1983 — 759-062/591

END

FILMED

1-84

DTIC